Dark Matter Study

Marieke van Beest

Ph 173 Research In Theoretical Physics

Advisors: Cliff Cheung, Maria Spiropulu

June 30, 2015



California Institute of Technology

Pasadena, California

Contents

1 Introduction **3**

2 Standard Cosmology **6**
2.1 A Brief History of the Universe 8
2.2 Thermal Production of Relics 8

3 Motivation from Particle Physics **10**

4 WIMPs **12**
4.1 The WIMP Miracle 12
4.2 The Supersymmetric Neutralino 14
4.3 Kaluza-Klein Dark Matter 16

5 Axions **18**

6 Asymmetric Dark Matter **19**

7 Dark Matter Detection **21**
7.1 Direct Measurements 22
7.1.1 WIMP Direct Detection 23
7.1.2 Axion Direct Detection 26
7.1.3 ADM Direct Detection 27
7.2 Indirect Measurements 27
7.2.1 WIMP Indirect Detection 28
7.2.2 ADM Indirect Detection 31
7.3 Colliders 32
7.3.1 WIMP Detection at the LHC 32
7.4 Astrophysical Probes 33
7.4.1 ADM Astrophysical Observations 33

8 Alternative Models **35**
8.1 MOND 35

9 Outlook **36**

References **36**

1 Introduction

Much effort has been put towards understanding the gravitational interactions of astronomical bodies since Isaac Newton published his *Principia* in 1687. This effort has occasionally resulted in the detection of anomalies where a celestial body deviates from its predicted trajectory. The detection of anomalies has been crucial to deepening our understanding of the Universe. If an anomaly is confirmed, it urges us to either revise our gravitational theory or else postulate the existence of hitherto undetected matter. A well-known historical example where the latter approach was successful is that of the conjectured existence of the planet Neptune based on deviations in the orbit of Uranus, which was first put forth by astronomers U. Le Verrier and J.C. Adams in 1846. Conversely, when the anomalous rate of precession of the perihelion of Mercury's orbit was attempted resolved by conjecturing the existence of the planet Vulcan, no such planet could be found, and the problem remained unsolved until the introduction of Einstein's General Theory of Relativity, for which it was a powerful motivation.

These historical cases are in many ways analogous to the modern problem of dark matter (DM), which was first postulated in 1933 by Fritz Zwicky [1]. In his article, *The Redshift of extragalactic Nebulae*, Zwicky argued based on his measurements of the velocity dispersion of galaxies in the Coma Cluster. Using the virial theorem to relate the dynamical mass of the Coma Cluster to the average speed (in the center-of-mass frame) of the constituent galaxies he concluded [1]: "In order to obtain the observed value of an average Doppler effect of 1000 km/s or more, the average density in the Coma system would have to be at least 400 times larger than that derived on the grounds of observations of luminous matter. If this would be confirmed we would get the surprising result that dark matter is present in much greater amount than luminous matter". Because Zwicky's measurements exceeded the luminosity in the solar neighborhood by two orders of magnitude he became the first to propose the existence of large quantities of non-luminous, dark matter.

On galactic scales the most convincing evidence of the existence of dark matter comes from measurements of rotation curves. The rotation curve of a galaxy is the graph of the circular velocities of stars and gas in the galaxy as a function of their distance from the galactic center. Rotation curves are usually observed to be flat at large distances (see Figure 1).

In Newtonian dynamics the circular velocity v as a function of the distance from the center of the rotational motion r is given by

$$v(r) = \sqrt{\frac{GM(r)}{r}}, \tag{1}$$

where $M(r) \equiv 4\pi \int \rho(r) r^2 dr$ and $\rho(r)$ is the mass density profile. The velocity should be falling as $\propto 1/\sqrt{r}$ outside the optical disc, seeing as $M(r)$ should be constant here. The fact that $v(r)$ is approximately constant implies $M(r) \propto r$ and hence $\rho(r) \propto 1/r^2$, which can be explained by the galaxy having a halo of non-luminous matter that extends well beyond the visible disc.

The DM hypothesis also provides a solution to the problem of instability in galactic disks. N-body simulations of the gravitational interactions of visible matter in flattened galaxies show that the disks are unstable, which disagrees with observations. This problem can be solved by assuming that galaxies have a halo of dark matter, which contributes gravitationally and stabilizes the disk [3].

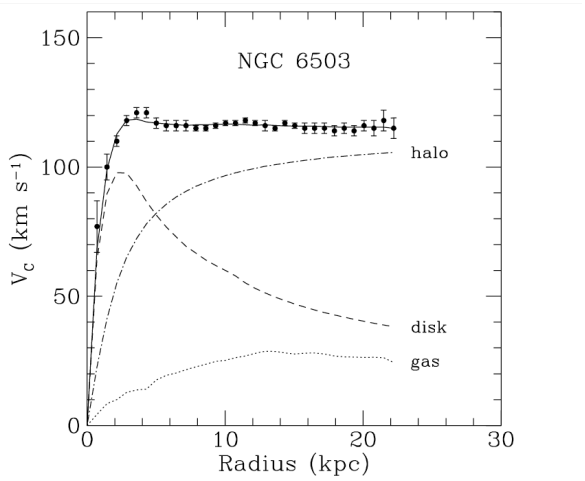


Figure 1: Rotation curve of NGC 6503. The dotted, dashed and dash-dotted lines are the contributions of gas, disk and dark matter, respectively. From Ref. [2].

Experiments based on gravitational lensing provide additional evidence for the existence of dark matter [2]. According to Einstein's gravitational theory, light propagates on geodesics, which deviate from straight lines when in a strong gravitational field. The distortion of images of background objects due to the gravitational field of a galaxy or cluster of galaxies can be used to infer its mass. This value can then be compared to the measure provided by the object's luminosity.

Some of the best current evidence for dark matter is provided by the Bullet cluster, which is a system where a subcluster is moving through a larger cluster at a relative speed of ~ 4500 km/s. In the Bullet cluster, the location of the baryonic matter, as determined using X-ray observations, is clearly shifted with respect to the gravitational potential, which was measured through weak lensing. The evidence from the Bullet Cluster strongly favors the DM hypothesis as opposed to a modification of the theory of general relativity [4].

Cosmological observations also support the existence of dark matter. Calculations based on the measured abundances of deuterium and helium imply that the baryonic fraction of the cosmological critical density is considerably smaller than one, $\Omega_b = \rho_b/\rho_c < 1$, where ρ_c is the average density needed to close the Universe [3] (see Section 2 for a discussion of the geometry of the Universe). From an aestethic point of view the prefered value for the total energy density is $\Omega = 1$. The argument is that this is the only value for which the energy density does not change rapidly with time. Observations to determine the geometry of spacetime indicate that the cosmological energy density is within an order of magnitude of unity today [5], implying for the energy density at the Planck time, $\Omega_{Pl} = 1 \pm 10^{-60}$, hence $\Omega = 1$ is the natural value. If the total energy density is different from unity it should change quickly with time, indicating that we live in a special time of the history of the Universe. The favored explanation is thus the existence of non-baryonic matter on cosmological scales.

The formation of large scale structure is also dependent on the dark matter hypothesis. Large scale structure formed from small density fluctuations in the early Universe. These fluctuations are measureable as temperaturevariations in the cosmic microwave background (CMB) radiation, [3] $\delta T/T \sim 10^{-4}$. Density perturbations grow during the matter-dominated epoch of the Universe (see Section 2), however, the measured variations are too small to allow for the formation of large scale structure

within the given time. This problem can also be solved by introducing additional matter in the form of non-interacting, non-baryonic particles.

So the hypothesis that dark matter exists is well motivated, but that does not answer the question of what dark matter is. All the above mentioned experimental methods rely on the gravitational interactions of dark matter for detection, and so do not provide us with much knowledge of the particle properties of dark matter.

It is natural to start searching for a candidate for dark matter within the standard model (SM) of particle physics that has, for many years and with great success, accounted for all observed particles and interactions. To be a good DM candidate the particle must be massive, electrically neutral, colorless and stable on the scale of the age of the Universe. Also, it must be phenomenologically viable, hence its predicted relic density must not exceed the constraints placed on it by experiments. The issue of thermal relic densities will be discussed in depth in Section 2.2 and for the case of WIMP dark matter in Section 4.1. The present energy densities of baryonic matter, non-baryonic dark matter and dark energy Λ are constrained to be [4]

$$\Omega_B \simeq 0.0456 \pm 0.0016. \tag{2}$$

$$\Omega_{DM} \simeq 0.227 \pm 0.014. \tag{3}$$

$$\Omega_\Lambda \simeq 0.728 \pm 0.015. \tag{4}$$

These are the three components that are expected to contribute to the total energy density of the Universe. Dark energy is the third and largest component which, unlike all matter, has repulsive gravitational interactions.

It is by no means assumed that dark matter is made up of a single particle species. Electrons can only contribute significantly to dark matter if neutralized by binding with protons, but the baryonic energy density Ω_B is too low for this to account for all dark matter. The remaining plausible DM candidates in the standard model are the neutrinos. But upper bounds on their masses imply that the neutrino relic density is [4] $\Omega_\nu \simeq \sum_i m_{\nu_i}/47\text{eV} \lesssim 0.012$, which is much too small for SM neutrinos to be a dominant part of dark matter. An additional argument against SM neutrinos comprising a major part of dark matter is that they would be highly relativistic at the time of freeze-out ($m_\nu/T_f \sim m_\nu/\text{MeV} \ll 1$), hence they would constitute hot dark matter, which is in conflict with observations of large scale structure.

As a consequence we are compelled to search for particle candidates for dark matter beyond the standard model. Fortunately, just as astronomers have traditionally postulated unseen matter, in particle physics there exists a tradition for inventing new particles, as when P.A.M. Dirac doubled the number of known particles by postulating the existence of antiparticles in 1930. Hence the initially astrophysical problem of dark matter has become one of the leading clues in the search for new physics beyond the standard model.

This report is organized as follows. The second section is a brief overview of standard cosmology, where relevant results and definitions from general relativity are presented. This section also contains a very condensed thermal history of the Universe, and a standard calculation illustrating the production mechanism for thermal relics. The third section presents problems in high energy physics that each motivate different dark matter particle candidates. Then follows three sections on the specific candidates or classes of candidate particles considered in this report. The fourth section examines

the favored WIMP scenario, and illustrates the WIMP miracle through a case study. Two WIMP candidates are contemplated, namely the supersymmetric neutralino and Kaluza-Klein dark matter. The fifth section concerns the axions and their non-thermal production mechanism, while the sixth section considers asymmetric dark matter. The seventh section studies the detection methods involved in the identification of the dark matter particle, their methodology and the constraints they impose. The types of detection considered are direct and indirect detection, particle colliders and astrophysical probes. An alternative to the dark matter hypothesis is contemplated in section eight, and, lastly, I contribute an outlook for the future of dark matter.

2 Standard Cosmology

The concept of dark matter arises within the context of the standard cosmological model whose fundamental picture is the Big Bang scenario. In this the Universe is described as having evolved by expansion from an extremely high-density state existing approximately 10^{10} years ago. This model allows us to explain in a satisfactory manner the thermal history of the Universe, the CMB, the abundance of elements, large scale structure and many other properties of the Universe.

The standard cosmological model exists within the framework of the theory of general relativity, in which it is specified in general by Einstein's equation, a specific form of the metric and the equation of state of the matter and energy of the Universe. Einstein's equation governs how the metric responds to energy and momentum analogous to Poisson's equation for the Newtonian gravitational potential:

$$\nabla^2\Phi = 4\pi G\rho. \tag{5}$$

Here Φ is the Newtonian potential, ρ is the mass density, and G is Newton's constant of gravitation. Einstein's equation can be arrived at by an argument involving generalizing the Poisson equation for the Newtonian potential to a tensorial equation as in [6] and by letting the metric play the role of the gravitational potential while the energy-momentum tensor plays that of the mass density. If conservation of energy is assumed, Einstein's equation appears as one of the simplest forms of a tensorial generalization of Poisson's equation for the Newtonian potential:

$$R_{\mu\nu} - \frac{1}{2}Rg_{\mu\nu} = 8\pi GT_{\mu\nu} + \Lambda g_{\mu\nu}. \tag{6}$$

In Einstein's equation $T_{\mu\nu}$ is the energy-momentum tensor which contains information of all the energy-like aspects of a system: energy density, pressure, stress, and so forth. $R_{\mu\nu}$ is the Ricci tensor (obtained by contraction of the Riemann curvature tensor), R is the Ricci scalar (the trace of the Ricci tensor), G is (still) Newton's constant of gravitation, and Λ is the cosmological constant, the value of the energy density of empty space. $g_{\mu\nu}$ is the metric which contains information of the geometry and causality of spacetime.

Contemporary cosmological models are based on the idea that the Universe is spatially isotropic and homogeneous. Isotropy states that space looks the same in any direction - it implies rotational invariance about a specific spatial point. The CMB supports this idea since its temperature fluctuations have been measured from our point in space to be on the order of 10^{-5}. Homogeneity is the statement that the

metric is the same throughout space and it implies translational invariance. These properties imply a specific form of the spacetime metric, called the Robertson-Walker metric:

$$ds^2 = -dt^2 + a^2(t)\left[\frac{dr^2}{1-kr^2} + r^2 d\Omega^2\right]. \tag{7}$$

$a(t)$ is called the scale factor and represents the relative expansion of the Universe in the sense that it measures the relative distance between cosmological objects at a time t relative to a reference time t_0. The value of k sets the curvature of the spatial surface. It can take on three values, $k = +1, 0, -1$. For k=+1 space is positively curved and is said to be *closed* (you can picture space as a higher dimensional sphere). For k=0 space has no curvature and is said to be *flat*. For k=-1 space has negative curvature and is said to be *open* (in this case you can imagine space as a higher dimensional hyperbola).

The matter and energy of the Universe is usually modeled as a perfect fluid and an equation of state, which relates pressure p and energy density ρ, is chosen. Often the perfect fluids relevant to cosmology obey

$$p = w\rho. \tag{8}$$

Here the assumption made about matter and energy consists in the fact that w is independent of time. Conservation of energy then determines the dependence of the energy density on the scale factor. In a universe whose energy density is mostly due to matter, which is said to be *matter-dominated*, the energy density falls off as $\rho_M \propto a^{-3}$. A universe in which most energy density is in the form of radiation is called *radiation-dominated* and for this $\rho_R \propto a^{-4}$. If an expanding universe has a non-zero vacuum energy this will eventually dominate the energy density because $\rho_\Lambda \propto a^0$. If this happens the Universe is called *vacuum-dominated*.

Einstein's equation determines the time evolution of the scale factor which is contained in the Friedmann equation

$$\left(\frac{\dot{a}}{a}\right)^2 = \frac{8\pi G}{3}\rho - \frac{k}{a^2}. \tag{9}$$

It is common to introduce the Hubble parameter

$$H(t) = \frac{\dot{a}(t)}{a(t)}. \tag{10}$$

The present value of the Hubble parameter is the Hubble constant [6] $H_0 = 70 \pm 10\ kms^{-1}Mpc^{-1}$. It is also useful to define the density parameter for a species i

$$\Omega_i = \frac{\rho_i}{\rho_c}, \tag{11}$$

and the total density of the Universe (in units of ρ_c)

$$\Omega = \sum_i \Omega_i = \sum_i \frac{\rho_i}{\rho_c}, \tag{12}$$

where the critical density is defined by

$$\rho_c = \frac{3H^2}{8\pi G}. \tag{13}$$

This quantity is called the critical density because the Friedmann equation can be put into the form

$$\Omega - 1 = \frac{k}{H^2 a^2}, \tag{14}$$

so that whether Ω is greater than, equal to, or less than one determines the sign of k and hereby the curvature of space.

2.1 A Brief History of the Universe

The key to the history of the Universe is understanding its history of expansion and cooling. In the following I provide a very brief summary of the thermal history of the Universe, which depends upon extrapolating our present knowledge of cosmology and particle physics back to the Planch epoch ($T \sim 10^{19}$ GeV) at which point quantum corrections to general relativity should render our current description of the Universe invalid. The following overview is based on Refs. [7] and [2].

At the earliest epoch the Universe was an extremely dense plasma of relativistic particles, including the quarks, leptons, gauge bosons and Higgs boson. According to current ideas, a number of spontaneous symmetry breaking (SSB) phase transitions occurred in the early Universe. The grand unification (GUT) phase transition is assumed to have occurred at a temperature of $T \sim 10^{14} - 10^{16}$ GeV at which some (unknown) grand unified group, G, breaks down into the SM gauge group, $SU(3) \otimes SU(2) \otimes U(1)$. The electroweak SSB phase transition takes place at a temperature of $T \sim 10^2$ GeV at which the SM gauge group breaks into $SU(3) \otimes U(1)$. At a temperature of $T \sim 10^1 - 10^3$ GeV weakly interacting dark matter candidates with masses on the scale of GeV-TeV (candidates that will be discussed in Section 4) *freeze out* and are left as a thermal relic. This mechanism will be discussed in the following section. The QCD phase transition occurs at a temperature of $T \sim 0.3$ GeV, after which the strongly interacting particles are bound in quark-triplet states (baryons) and quark-antiquark states (mesons). At a temperature of $T \sim 10^2$ keV the much better understood process of Big Bang nucleosynthesis (BBN) takes place and the light elements are produced. The BBN provides the most stringent constraints to the Big Bang theory, and the agreement between observations and the BBN predictions for the abundances of light elements is remarkable. At $T \sim 1$ eV the matter density becomes equal to that of radiation and the current matter-dominated epoch of the Universe commences. This point also marks the beginning of the formation of structure in the Universe. At a temperature of $T \sim 0.4$ eV atoms begin to form and the photons of the Universe decouple from the matter, producing the cosmic background radiation. The present temperature of the Universe (or of the CMB) is $T = 2.7$ K $\sim 10^{-4}$ eV.

2.2 Thermal Production of Relics

For all practical purposes, the Universe has for much of its history been in thermal equilibrium. When a particle species is in local thermal equilibrium it is constantly

produced as well as destroyed. For the case of a dark matter particle interacting with standard model particles, reactions like, DM DM $\rightarrow$ SM SM, decrease the number of DM particles, and reactions like, SM SM $\rightarrow$ DM DM, increase the number of DM particles. The respective processes of creation and destruction are equally efficient as long as the temperature is higher than the mass of the DM particle, $T \gtrsim m_{DM}$. When the temperature reaches the order of m_{DM} the reaction which produces DM particles becomes Boltzmann suppressed and the number density n of the DM particles is then given by

$$n_{DM,eq} = g_{DM} \left(\frac{m_{DM} T}{2\pi} \right)^{3/2} e^{-m_{DM}/T}. \tag{15}$$

Here g_{DM} is a measure of the relativistic degrees of freedom of the DM particles given in Ref. [7]. As can be seen from the above expression the abundance of dark matter would quickly have diminished had it stayed in thermal equilibrium. A thermal relic is produced because of the Hubble expansion. When the expansion rate of the Universe starts to dominate over the annihilation rate of the dark matter, the DM particles cease to interact with one other and decouple from the thermal plasma of the Universe. The process of thermal freeze-out is described quantitatively by the Boltzmann equation

$$\frac{dn}{dt} = -3Hn - \langle \sigma_A v \rangle \left(n^2 - n_{eq}^2 \right), \tag{16}$$

where H is the Hubble parameter, $\langle \sigma_A v \rangle$ is the thermally averaged DM annihilation cross-section, and n_{eq} is the DM number density at equilibrium. The three terms on the right-hand side of eq. 16 account respectively for the expansion of the Universe, particle annihilation and creation. If particles were neither created nor destroyed ($\langle \sigma_A v \rangle = 0$), the number density of DM particles would decrease only due to the Hubble expansion as $n \sim a^{-3}$. The n^2 term also gives rise to a decrease in number density which is due to annihilation of dark matter to SM particles. With only annihilation the number density is exponentially suppressed, $n \sim e^{-t/t_A}$, then $dn/dt = -n/t_A = -\langle \sigma_A v \rangle n^2$ with a typical annihilation time $t_A \simeq 1/\langle \sigma_A v \rangle n$. The n_{eq}^2 term causes an increase in number density which is due to the reverse process in which DM particles are created from SM particles.

Eq. 16 can be put into a more useful form by introducing the variables

$$Y \equiv \frac{n}{s}, \quad Y_{eq} \equiv \frac{n_{eq}}{s}, \tag{17}$$

$$x \equiv \frac{m_{DM}}{T}, \tag{18}$$

where $s = 2\pi^2 g_{*S} T^3/45$ is the entropy density. The entropy per comoving volume is conserved, $sa^3 = constant$, which means that Y is proportional to the number of particles per comoving volume, $Y \propto na^3$. It also implies $\dot{s} = -3Hs$, such that

$$\frac{dY}{dt} = (\dot{n} + 3Hn)/s, \tag{19}$$

and, with a change of differentiation variable, the Boltzmann equation then takes the form

$$\frac{dY}{dx} = \frac{1}{3H} \frac{ds}{dx} \langle \sigma_A v \rangle (Y^2 - Y_{eq}^2). \tag{20}$$

Substituting eq. 9 with $k = 0$ for the Hubble parameter with $\rho = g_*\pi^2 T^4/30$, the following equation can then be obtained

$$\frac{dY}{dx} = -\lambda x^{-2}\left(Y^2 - Y_{eq}^2\right), \tag{21}$$

where $\lambda = 0.264(g_{*S}/g_*^{1/2})m_{DM}m_{Pl}\langle\sigma_A v\rangle$, and $Y_{eq} = 0.145(g/g_{*S})x^{3/2}e^{-x}$. Here m_{Pl} is the Planck mass, and $g_* \approx g_{*S}$ count the relativistic degrees of freedom of all plasma in the Universe. They are given in Ref. [7]. Parameterizing the thermally averaged annihilation cross-section as $\langle\sigma_A v\rangle = \sigma_0 x^{-n}$, the equation can be solved approximately for the present value of Y:

$$Y_0 = \frac{3.79x_f}{\frac{g_{*S}}{g_*^{1/2}}m_{DM}m_{Pl}\sigma_0}, \tag{22}$$

$$Y_0 = 3.81\times10^{-18}\ \text{GeV}\times\frac{100\ \text{GeV}}{m_{DM}}\times\frac{x_f}{40}\times\frac{0.01\ \text{GeV}^{-2}}{\sigma_0}, \tag{23}$$

realistic value?where

$$x_f = \ln\left[0.038\frac{g}{g_*^{1/2}}m_{DM}m_{Pl}\sigma_0\right] - \frac{1}{2}\ln\left\{\ln\left[0.038\frac{g}{g_*^{1/2}}m_{DM}m_{Pl}\sigma_0\right]\right\}. \tag{24}$$

In the above, x_f denotes x at freeze-out. The relic density is then given by

$$\Omega_{DM} = \frac{m_{DM}Y_0 s_0}{\rho_c}, \tag{25}$$

where s_0 is the present entropy density. The above results will be used in a case study of the thermal relic of a WIMP in Section 4.1.

The time evolution of Y, which is essentially the relic density, is obtained by solving the Boltzmann equation numerically. The solution is illustrated in Figure 2. Notice that at freeze-out, the actual abundance departs from the equilibrium value and remains constant while the equilibrium value falls off rapidly. The dependence of the relic density on the thermally averaged annihilation cross-section is also illustrated. With a greater cross-section the DM particles annihilate at a greater rate and thus are more depleted at freeze-out leading to a smaller constant relic density subsequent to freeze-out.

Notice that in the above analysis I have assumed that the dark matter is in thermal equilibrium before decoupling, that the DM particle is stable, that the DM particles can only be destroyed and created in pairs, and that there is no asymmetry between DM particles and anti-DM particles. **Do other assumptions go into this analysis?**

3 Motivation from Particle Physics

A number of popular models exist that provide candidates for the constituents of dark matter. Remarkably, these theories were usually conceived to solve problems profoundly different from the astrophysical one of dark matter. This is because the observations of missing matter are not the only motivation for new physics beyond the standard model. Another important incentive exists within particle physics, namely

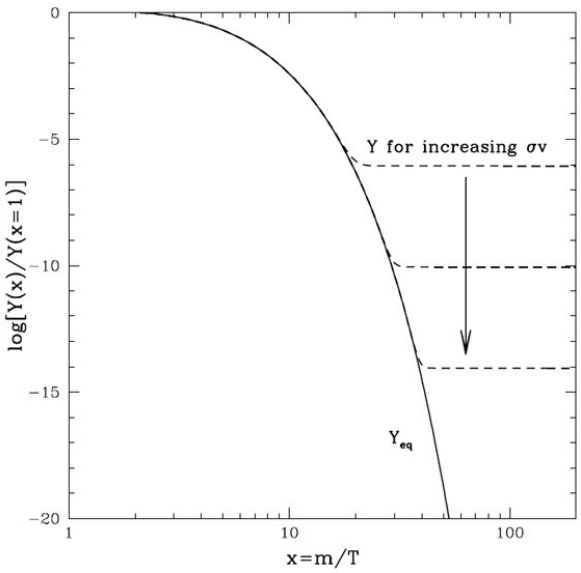


Figure 2: Result of numerical integration of the Boltzmann Equation. The solid line is the equilibrium value and the dashed line is the actual abundance (indicated for different annihilation cross sections σv). Adapted from Ref. [7].

the so-called "fine-tuning" problems of the standard model.

Problems of fine-tuning refer to instances where seemingly unnatural choices of parameters are necessary for the standard model to be able to explain experimental data. The *gauge hierarchy problem* is one such instance. It is also the leading motivation for a specific class of dark matter candidates, the weakly interacting massive particles, WIMPs.

The gauge hierarchy problem concerns the size of the mass of the Higgs boson [8] $m_h = 126.0 \pm 0.4$ (stat) ± 0.4 (sys) GeV. The Higgs mass is a dimensionful parameter, and any dimensionful parameter of the standard model is expected to either be 0, if enforced by a symmetry, or of a natural scale defined by the three known fundamental constants of nature: Planck's constant h, the speed of light c, and Newton's gravitational constant G. A unique combination of these three constants exists that has dimensions of mass, namely the Planck mass $m_{Pl} \equiv \sqrt{hc/G} \simeq 1.2 \times 10^{19}$ GeV. The gauge hierarchy problem is the question of why $m_h \ll m_{Pl}$.

The physical mass of the Higgs boson is $m_h^2 = m_{h0}^2 + \delta m_h^2$, where m_{h0}^2 is the tree-level mass and $\delta m_h^2 \sim \Lambda^2/16\pi^2$ is the loop-level quantum correction[1] [4]. Λ is the energy scale at which the standard model breaks down. Because δm_h^2 is proportional to Λ^2, the correction is expected to bring the Higgs boson mass up to within an order of magnitude of Λ. With $\Lambda \sim m_{Pl}$, this implies that m_{h0}^2 and δm_h^2 must cancel to 1 part in 10^{36} for the Higgs mass to have the experimentally determined value.

The gauge hierarchy problem can be solved by assuming that $\Lambda \lesssim 1$ TeV. Then the Higgs mass will only be expected to be pulled up to within an order of magnitude of 1 TeV by the quantum corrections, which is consistent with experiments. This implies new physics at the weak scale $m_{weak} \sim 10$ GeV-TeV, and thus new particles with

[1] "Tree-level" and "loop-level" is quantum field theory (QFT) terminology and refers to Feynman diagrams. Tree-like Feynman diagrams give the leading order terms in perturbation theory, while loop diagrams contribute corrections with one factor of $\hbar$ for each loop.

masses around m_{weak}. These particles could be the constituents of dark matter.

A different fine-tuning problem that motivates a certain kind of DM candidate is the *strong CP problem*. CP-symmetry (Charge Parity symmetry) is the statement that the laws of physics are invariant under the combined application of charge conjugation and parity. That is, antimatter should behave exactly the same as matter with the spatial directions reversed. The strong CP problem is the question of why QCD does not seem to break CP-symmetry, when a violation of the symmetry is possible within QCD.

The QCD part of the SM Lagrangian includes the term [4] $g_3^2\theta_3/(32\pi^2)\epsilon^{\mu\nu\rho\sigma}G^{\alpha}_{\mu\nu}G^{\alpha}_{\rho\sigma}$, where g_3 is the coupling of the strong interactions, $G_{\mu\nu}$ is the gluon field strength and $\epsilon^{\mu\nu\rho\sigma}$ is the totally anti-symmetric tensor. The strength of this term is characterized by the angle parameter θ_3. The term contributes to CP-violating, flavor-conserving observables, such as the electric dipole moment (EDM) of the neutron d_e. For a natural choice of $\theta_3 \sim 1$, one expects $d_e \sim 10^{-16}e$ cm. However, a non-zero experimental value for the neutron electric dipole moment has not yet been observed, and it is already constrained by experiment to [4] $d_e < 2.9 \times 10^{-26}e$ cm. This implies $\theta_3 \sim 10^{-10}$, and thus constitutes a fine-tuning problem of 1 part in 10^{10}. A solution to the strong CP problem exists that predicts new particles, axions, that are possible DM candidates.

4 WIMPs

WIMP dark matter candidates are stable particles that interact through the weak force and gravity, but that are colorless and electrically neutral. They have masses of $m_{weak} \sim 10$ GeV-TeV. Many beyond the SM theories predict the existence of WIMPs. In addition to solving the gauge hierarchy problem, another strong motivation for WIMP dark matter is that they are naturally produced in the correct amount through thermal production. This fortuity, accommodating both astrophysics and particle physics so nicely, has been dubbed the *WIMP miracle*.

4.1 The WIMP Miracle

The following is a case study that illustrates the WIMP miracle. The model used is that of a DM sector, which is a carbon copy of electromagnetism. Concretely, the DM is modeled as a "dark electron" of mass m_{DM} with charge q_{DM} under a "dark force" mediated by a "dark photon".

The annihilation cross-section of dark matter into dark photons can be roughly estimated by appropriately altering the expression for the cross-section of electron-positron annihilation into regular photons. This cross-section is given by [9]

$$\sigma = \pi\left(\frac{\alpha\hbar}{m_e c}\right)^2 \frac{1}{\gamma-1}\left\{\frac{\gamma^2+4\gamma+1}{\gamma^2-1}\ln\left(\gamma+\sqrt{\gamma^2-1}\right) - \frac{\gamma+3}{\sqrt{\gamma^2-1}}\right\}. \qquad (26)$$

In the above equation $\alpha = e^2/\hbar c$ is the coupling constant, $\gamma = E/m_e c^2$ where E is the energy of the incoming positron (electron is assumed initially at rest), m_e is the mass of the electron and e is its charge. This equation will describe the dark matter model under consideration here if we let $m_e \to m_{DM}$, and $e \to q_{DM}$, so that $\alpha \to \alpha_{DM} = \frac{q_{DM}^2}{\hbar c}$, and $\gamma \to \frac{E}{m_{DM}c^2}$. To simplify the treatment I will work in natural units from this point

forward.
In the low energy limit,

$$\gamma \simeq 1 + \frac{E_{kin}}{m_{DM}} = 1 + \frac{3}{2}\frac{1}{x}, \tag{27}$$

Where E_{kin} is the non-relativistic kinetic energy of the incoming particle and $x = m_{DM}/T$, where T is the temperature of the DM sector. In this limit, eq. (26) can be approximated to

$$\sigma \simeq \pi \left(\frac{\alpha_{DM}}{m_{DM}}\right)^2 \frac{4x^{3/2}}{3\sqrt{3}}. \tag{28}$$

If we assume the DM sector was in thermal equilibrium before freeze-out, referring back to Section 2.2, the relic density of the dark matter is given by

$$\Omega_{DM} = \frac{m_{DM} Y_0 s_0}{\rho_c}, \tag{29}$$

where,

$$Y_0 = \frac{3.79 x_f}{\frac{g_{*S}}{g_*^{1/2}} m_{DM} \sigma_0}, \tag{30}$$

$$x_f = \ln\left[0.038 \frac{g}{g_*^{1/2}} m_{DM}\sigma_0\right] - \frac{1}{2}\ln\left\{\ln\left[0.038 \frac{g}{g_*^{1/2}} m_{DM}\sigma_0\right]\right\}. \tag{31}$$

At electron-positron freeze-out [7] $g_* \simeq 11$ and $g = 4$ for this scattering process.

Combining the expressions for the annihilation cross-section and x at freeze-out, eqs. (28) and (31), we obtain

$$x_f = \ln\left[1.35 \cdot 10^{18}\ \frac{\alpha_{DM}^2 x^{3/2}}{m_{DM}}\right] - \frac{1}{2}\ln\left\{\ln\left[1.35 \cdot 10^{18}\ \frac{\alpha_{DM}^2 x^{3/2}}{m_{DM}}\right]\right\}. \tag{32}$$

For $m_{DM} \sim m_{weak} \sim 100$ GeV and [4] $\alpha_{DM} \simeq 0.65$ this gives $x_f \simeq 40$.

Using the expression for the annihilation cross-section, eq. (28), in the expression for Y_0, eq. (30), we obtain

$$Y_0 = \frac{0.47 m_{DM}}{\alpha_{DM}^2 x_f^{1/2}}. \tag{33}$$

The dark matter then has a relic density of

$$\Omega_{DM} = \frac{1.3 \cdot 10^8 m_{DM}^2}{\alpha_{DM}^2 x_f^{1/2}} \mathrm{GeV}^{-1}. \tag{34}$$

Evidently the relic density is proportional to the inverse square of the DM coupling constant, $\Omega_{DM} \propto \alpha_{DM}^{-2}$. This result is in agreement with the heuristic argument that if the dark matter is strongly coupled, it will have a larger cross-section and annihilate more, hence there will be less dark matter left at the time of freeze-out and the relic

density will then be smaller. Now, x_f changes with the logarithm of m_{DM}. If $x_f \simeq 40$ is regarded as a constant the relic density is proportional to the square of the DM mass,

$$\Omega_{DM} = \frac{2.1 \cdot 10^7 m_{DM}^2}{\alpha_{DM}^2} \text{GeV}^{-1}. \tag{35}$$

The experimentally determined DM relic density is [4] $\Omega_{DM} = 0.227 \pm 0.014$. This value is saturated for

$$\alpha_{DM}^2 = 9.1 \cdot 10^7 m_{DM}^2 \text{GeV}^{-1}. \tag{36}$$

From this expression it is evident that the DM charge must scale with the DM mass as $q_{DM} \sim m_{DM}^{1/2}$. If we assume that the dark matter interacts weakly, $\alpha_{DM} \leq 1$, then the DM mass is bounded by

$$m_{DM} \leq 3.7 \cdot 10^5 \text{ GeV}. \tag{37}$$

This result tells us that to saturate the experimentally determined DM relic density with a weak DM coupling, the mass of the dark matter should be smaller than $m_{DM} \lesssim 100$ TeV. This is what is know as the WIMP miracle! That weakly interacting particles of mass $m_{weak} \sim 10$ GeV-TeV naturally give the observed relic density.

4.2 The Supersymmetric Neutralino

A popular WIMP dark matter candidate comes from the framework of supersymmetry (SUSY), which is a theoretically appealing extension of the standard model that introduces a symmetry relating the fundamentally distinct particle species of bosons and fermions. In the standard model, bosons are the force mediators with integer spins, and fermions are the constituents of matter with half-integer spins. In SUSY, every SM particle gets a supersymmetric partner, which has the same quantum numbers and gauge interactions, but which differs in spin by 1/2, thus providing a more aesthetically appealing symmetric picture of matter and interactions. However, these superpartners have yet to be observed experimentally.

Supersymmetry elegantly solves the gauge hierarchy problem, because the introduction of partners with opposite spin statistics contributes with opposite signs to the quantum corrections to the Higgs mass [4]

$$\delta m_h^2 \sim \frac{1}{16\pi^2} \left(m_{SUSY}^2 - m_{SM}^2 \right) \ln \frac{\Lambda}{m_{SUSY}}, \tag{38}$$

where m_{SM} and m_{SUSY} are the masses of the SM particles and their superpartners. For $m_{SUSY} \sim m_{weak}$ this is at most an $\mathcal{O}(m_{h0}^2)$ correction, even with $\Lambda \sim m_{Pl}$. The gauge hierarchy problem has thus been solved, given that the superpartners have weak scale masses. A number of models for supersymmetry breaking exist, which generate this scenario.

Another theoretical motivation for supersymmetry is that it enables the unification of the gauge coupling parameters at a scale $M_U \sim 2 \times 10^{16}$ GeV, as illustrated in Figure 3. Extrapolation of the coupling constants using only the standard model fails to unify them at a common value. Introducing supersymmetry at the TeV scale, the

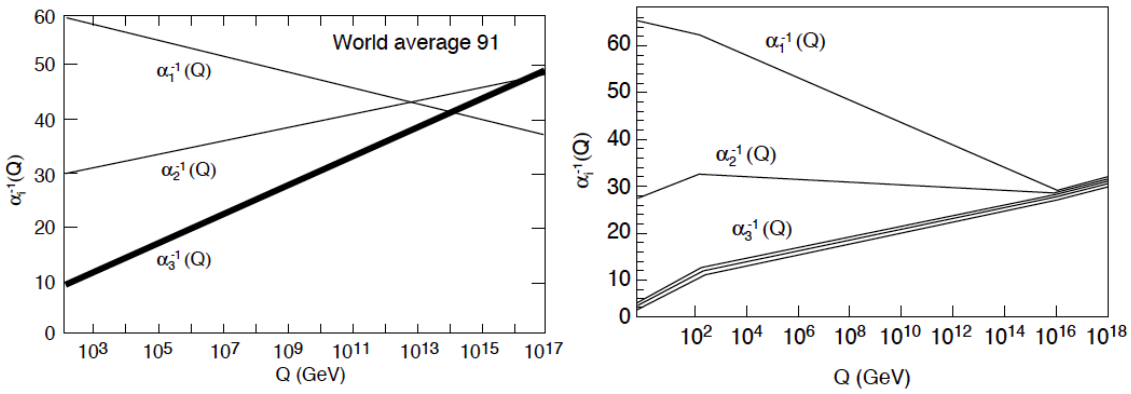


Figure 3: Extrapolation of measurements of the gauge coupling strengths at LEP using only the standard model (left), including supersymmetry (right) [2].

forces naturally unify to a high accuracy at the scale of M_U. This has been taken as a strong indication in favor of a grand unified theory, in which the fundamental forces are unified below the Planck scale.

From the perspective of dark matter, in any supersymmetric model that conserves R-parity the lightest superpartner (LSP) will be naturally stable over cosmological timescales. R-parity is defined as $R = (-1)^{3B+L+2S}$, where B denotes baryon number, L denotes lepton number, and S denotes spin. All SM particles have $R = 1$ parity, while all superpartners have $R = -1$. R-parity conservation stabilizes the LSP, since it is impossible for it to decay to something with a smaller mass and R-parity -1.

The identity of the LSP depends on the hierarchy generated by the model specific mechanism for supersymmetry breaking. If SUSY were not broken, each superpartner would have the same mass as its SM counterpart, which is clearly not the case. For dark matter, it is natural to search for the LSP among the electrically neutral and colorless superpartners. In the minimal supersymmetric standard model (MSSM), which is minimal in the sense that it contains the smallest possible field content in order to give rise to all the SM fields, this list is limited to,

Spin 3/2 fermion: Gravitino, $\tilde{G}$
Spin 1/2 fermions: $\tilde{B}, \tilde{W}, \tilde{H}_u, \tilde{H}_d \rightarrow$ Neutralinos $\tilde{\chi}_1, \tilde{\chi}_2, \tilde{\chi}_3, \tilde{\chi}_4$
Spin 0 scalars: Sneutrinos, $\tilde{\nu}_e, \tilde{\nu}_\mu, \tilde{\nu}_\tau$.

The gravitino is the superpartner of the hypothetical mediator of gravity within QFT, the spin 2 graviton. The gravitino is not a WIMP but it is a viable DM candidate, however, one that will not be discussed further in this report.

The sneutrinos are predicted to annihilate and scatter very efficiently, and consequently they have been ruled out as DM candidates either because they are under abundant or excluded by direct detection experiments. In the context of direct detection, the Feynman diagram corresponding to sneutrino annihilation into quarks can be turned on its side to produce a scattering diagram. The scattering cross section of this reaction has been computed for a $\sim 100 - 1000$ GeV sneutrino and it turns out to be several orders of magnitude greater than experimental constraints [10]. Accordingly, sneutrinos have been abandoned as DM candidates.

The bino, $\tilde{B}$, and the wino, $\tilde{W}$, are the superpartners of the B and W_3 gauge bosons (or, equivalently, the photon and Z). Supersymmetric models require two Higgs bosons

of which the higgsinos, $\tilde{H}_u$ and $\tilde{H}_d$, are the superpartners. These four sparticles (the rather brilliant term for a general superpartner) combine to form four physical mass eigenstates, namely the four neutralinos. The neutralinos are typically labeled as illustrated above, in order of increasing mass. The lightest one is usually referred to simply as *the neutralino* and is labeled by $\tilde{\chi}$. It can annihilate through numerous Feynman diagrams. Which reaction dominates in the process of thermal production depends on the composition of the neutralino along with a large number of other parameters. These circumstances make the neutralino relic density very difficult to calculate accurately.

Although the MSSM is relatively simple, it still has an excessive amount of unknown parameters for phenomenological purposes. To make progress, the number of parameters must be reduced by making justified simplifying assumptions. Conclusions based on the simplified model can then be generalized to a certain extend. The canonical model for the study of supersymmetry is minimal supergravity (mSUGRA or constrained MSSM) in which a number of parameters are assumed to unify at the grand unification scale. Respectively, these parameters are the gauge coupling constants, the gaugino masses, the scalar masses (sfermions and Higgs bosons), and the trilinear couplings. The number of free parameters is then reduced to as little as four and a sign:

$$\tan\beta,\ M_{1/2},\ m_0,\ A_0,\ \mathrm{sign}(\mu)$$

Here $\tan\beta$ is the ratio of the vacuum expectation values of the two Higgs fields, $M_{1/2}$ is the unified gaugino mass, m_0 is the unified scalar mass, and μ is the higgsino mass parameter. For all but the most extreme values of $\tan\beta$ and A_0, m_0 and $M_{1/2}$ dominate the collider and DM phenomenology. In Figure 4 is shown a region of mSUGRA parameterspace for fixed values of $\tan\beta$, A_0, and $\mathrm{sign}(\mu)$. It is evident from Figure 4 that the current constraints on the DM relic density Ω_{DM} are highly constraining since the cosmologically favored region is approximately reduced by one dimension compared to the parameterspace $(m_0, M_{1/2})$. Of course, in other regions of the mSUGRA parameterspace other points in the $(m_0, M_{1/2})$ plane are cosmologically viable.

4.3 Kaluza-Klein Dark Matter

New weak scale physics is also to be found in theories with extra dimensions. Although our world seems to be made up of 3+1 dimensions (three spatial and one time), theories exist which postulate the appearance of extra dimensions at higher energy scales. The idea first received attention in 1921, when Kaluza applied it in an attempt to unify electromagnetism and gravity. This original application turned out not to be viable, but the concept exists in many contemporary forms.

The study of theories with extra dimensions is motivated by *string theory* and *M-theory*, which today appear to be the best candidates for a consistent description of quantum gravity. These theories seem to require six or seven extra dimensions. In addition, the gauge hierarchy problem can be addressed in this formalism, but not all extra dimension theories resolve the gauge hierarchy problem. The ones that do not are assumed to be low-energy approximations to more complete theories.

A class of higher dimension theories are those with universal extra dimensions (UED), in which all particles and fields of the standard model can propagate in the

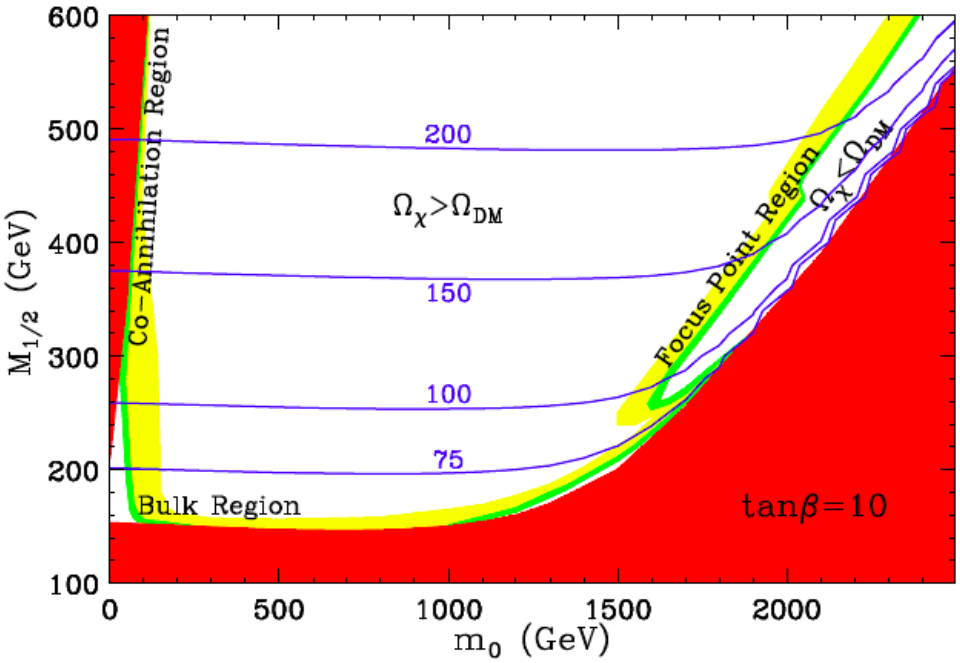


Figure 4: Region of mSUGRA $(m_0, M_{1/2})$ parameterspace for $\tan\beta = 10$, $A_0 = 0$, $\mu > 0$. The green (yellow) region is cosmologically favored with a neutralino relic density, $0.20 < \Omega_{\tilde{\chi}} < 0.28$ $(0.2 < \Omega_{\tilde{\chi}} < 0.6)$. The names of cosmologically favored regions are indicated (Co-Annihilation Region, Bulk Region, Focus Point Region), as well as regions with too small and too large neutralino relic densities. The lower right red shaded region is excluded by collider bounds on chargino masses, and the upper left red region is excluded by the presence of a stable charged particle. Contours for the neutralino mass $m_{\tilde{\chi}}$ in GeV are shown as blue lines. From Ref. [4].

extra dimensions, as opposed to some or all the SM fields being confined to a brane imbedded in the higher dimensional spacetime. UED theories contain small, compact, flat extra dimensions. They provide an attractive dynamical mechanism for electroweak symmetry breaking, prevent rapid proton decay and *contain a viable WIMP dark matter candidate*.

A general feature of extra dimension theories is that compactification of the extra dimensions gives rise to so-called Kaluza-Klein (KK) states. These appear in four dimensions as a series (called a tower) of states with masses $m_n = n/R$, where n labels the KK level and R characterizes the size of the extra dimension. UED models preserve a discrete parity called KK-parity. In much the same way as R-parity stabilizes the LSP, KK-parity ensures that the lightest (first level) KK particle (LKP) is stable.

In the simplest UED model, minimal UED, there is one extra dimension compactified on a circle, with y and $-y$ identified, where y is the coordinate of the extra dimension. Every SM particle has an infinite number of partner particles, one at each KK level, all of which have the same quantum numbers, but which differ in mass as indicated above. The parameterspace of minimal UED is extremely simple, depending only on the Higgs mass $m_h = 126.0 \pm 0.4$ (stat) ± 0.4 (sys) GeV and the compactification scale of the extra dimension R. The constraint on the size of the extra dimension from precision electroweak measurements is [2] $R^{-1} \gtrsim 300$ GeV, making the KK particle masses close to weak scale.

The LKP is typically B^1, the level one partner of the hypercharge gauge boson. It is electrically neutral, colorless, and stable because of KK-parity. KK dark matter masses from approximately 500 GeV to several TeV can potentially lead to relic densities consistent with measurements.

5 Axions

Axions were introduced in an attempt to solve the strong CP problem of particle physics, and have since been proposed as a DM candidate. The axion model introduces a new pseudoscalar field A into the SM Lagrangian. The axion Lagrangian term is [4]

$$\mathcal{L}_A = -\frac{g_3^2}{32\pi^2}\frac{A}{f_A}\epsilon^{\mu\nu\rho\sigma}G^{\alpha}_{\mu\nu}G^{\alpha}_{\rho\sigma}. \tag{39}$$

The axion term is inversely proportional to f_A, the axion decay constant, which sets the mass of the axion. With the introduction of the axion field, the angle parameter θ_3 of the strong CP problem effectively becomes dynamical with a dependence on A and f_A. This allows for the angle parameter to relax to a minimum, $\theta_3 \to 0$, such that the predicted electric dipole moment of the neutron is small enough to be consistent with current bounds (see Section 3 for a discussion of the problem of CP violation and the size of the neutron EDM).

The axion is the particle associated with excitations about the minimum at $\theta_3 = 0$. All its couplings are suppressed by inverse factors of the axion decay constant, which is typically expected to be of order $f_A \sim 10^{12}$ GeV in the axion DM scenario, because this yields [11] $\Omega_A \sim 1$. Axions couple to ordinary matter and gluons, and have loop-level interactions with photons. The axion solution to the strong CP problem works equally well for all values of the axion decay constant, and hence for all values of the axion mass. However, stability considerations and experimental constraints imply that axions are extremely weakly interacting and light, at least twelve orders of magnitude lighter than WIMPs. The axion mass and interactions are determined by f_A up to model-dependent constants. The axion mass is [11]

$$m_A = \frac{\sqrt{m_u m_d}}{m_u + m_d} m_\pi f_\pi \frac{1}{f_A} \approx 6\ \mu\text{eV} \times \frac{10^{12}\ \text{GeV}}{f_A}, \tag{40}$$

where $m_u \simeq 4$ MeV, $m_d \simeq 8$ MeV are the masses of the up and down quarks respectively, and $m_\pi \simeq 135$ MeV, $f_\pi \simeq 93$ MeV are the mass and the decay constant of the pion.

Axions are assumed to be produced through a non-thermal mechanism, one which was proposed by J. Preskill, M. Wise and F. Wilczek [11]. Axion DM cannot be accounted for by standard thermal production, because thermally produced axions would have a relic density of [4] $\Omega_A^{th} \sim 0.22(m_A/80\ \text{eV}) \lesssim 10^{-5}$, which is much too small for axions to make up a significant amount of the observed dark matter. Axion production is related to the spontaneous breaking of the Peccei-Quinn (PQ) symmetry, which occurs at the scale f_A. With the PQ phase transition the axion field acquires several minima into which the field can relax. Regions that are not causally connected do not necessarily reside in the same minima, and the resulting axion field may consist of several patches with different field values. These domains and the walls separating them have not been observed, which motivates the assumption that the PQ symmetry

is broken prior to inflation. The exponential expansion of the inflationary epoch may stretch a single valued patch of the axion field to include the entire visible Universe. However, there is no reason for the expectation value of the field $\langle A \rangle$ to be at the minimum when the axion freezes out. On the contrary, the typical value expected is $\langle A \rangle \sim f_A$. Consequently, potential energy will be stored in the field and it will begin to oscillate about the minimum. These oscillations represent the axion energy density of the Universe. It has been shown that if this energy density is not dissipated through the Hubble expansion, it will overclose the Universe. The condition for the axion energy density to be sufficiently dissipated by the Hubble expansion to not exceed the critical density is [11] $f_A \lesssim 10^{12}$ GeV, or equivalently $m_A \gtrsim 6$ μeV.

By considering the loop-level interactions of axions with photons, one arrives at the implication that for axions to be stable over the lifetime of the Universe their mass is constrained by [4] $m_A \lesssim 20$ eV. Even more stringent upper bounds on the axion mass have been provided by a variety of laboratory and astrophysical experiments, implying [11] $m_A \lesssim 6$ meV, or equivalently $f_A \gtrsim 10^9$ GeV.

Summarizing, the most stringent constraints imposed on the axion decay constant and, correspondingly, on the axion mass are

$$10^{12} \text{ GeV} \gtrsim f_A \gtrsim 10^9 \text{ GeV} \tag{41}$$

$$6\ \mu\text{eV} \lesssim m_A \lesssim 6 \text{ meV}. \tag{42}$$

6 Asymmetric Dark Matter

Asymmetric Dark Matter is based on the idea that instead of DM being thermally produced, as in the canonical WIMP scenario, the DM has its origin in a particle-anti-particle asymmetry similar to that of baryons. This idea is motivated by the fact that the density of baryons and the density of DM in the Universe are very close to one another [12]

$$\Omega_{DM}/\Omega_B \approx 5. \tag{43}$$

In the case of thermal production this is viewed as a mere coincidence, since the parameters determining the baryon density and the DM density are completely uncorrelated. The asymmetric DM scenario takes advantage of baryons and DM having similar production mechanisms and relates the baryonic asymmetry to the DM asymmetry providing an *a priori* reason for the similarity of the densities. Because the ADM density is set by its asymmetry, which is directly related to the baryon asymmetry, this implies [12]

$$n_X - n_{\bar{X}} \sim n_b - n_{\bar{b}}, \tag{44}$$

where n_X, $n_{\bar{X}}$ are the number densities for DM and anti-DM, and n_b, $n_{\bar{b}}$ are the number densities for baryons and anti-baryons. Throughout this section the DM particles will be denoted by X. The relation in eq. (43) then suggests, $m_X \sim 5 m_p \simeq 5$ GeV, though the DM mass may deviate from this value by a factor of a few depending on the details of the model.

The ADM mechanism works by initially creating an asymmetry either in the visible sector, dark sector or in both simultaneously. One way of obtaining similar asymmetries in the dark and visible sectors is strongly associated with existing baryo- and

leptogenesis models. Making use of this existing asymmetry in baryons and leptons, the theory is comprised of the *transfer* mechanism that communicates the asymmetry in visible matter to the dark sector. Alternatively, the *generation* of the asymmetry can involve the DM. There are two possible scenarios in which this is the case: *cogenesis*, where the asymmetry is generated simultaneously in the dark and visible sectors, or *darkogenesis*, where the asymmetry is generated exclusively in the dark sector and then transferred to the visible matter.

Two distinct transfer mechanisms have been proposed for sharing a primordial dark or baryon asymmetry. One makes use of electroweak sphalerons, which are known to violate baryon (B) and lepton (L) number in the standard model. In sphaleron transfer models, the DM particle carries a global Dark number D analogous to baryon and lepton number. The associated symmetry may be violated via sphalerons. It can be shown that sphalerons violate $B + L + \frac{N_X}{N_g} D$ and conserve $B - L$ and $B - \frac{N_g}{N_X} D$, where N_g is the number of generations carrying B and L, and N_X is the number of DM electroweak doublets, thus $\frac{N_g}{N_X}$ is a positive rational number. This implies that it is possible to have a reaction that converts N_g baryons (anti-baryons) into N_X anti-DM particles (DM particles). The DM number will then freeze in when the electroweak sphalerons decouple. The other mechanism for transferring a primordial dark or baryon asymmetry makes use of higher dimension operators and renormalizable interactions. The basic idea of this mechanism is to add terms to the Lagrangian that correspond to interactions between the DM particles and SM particles mediated by a heavy field. These interactions will then be important in the high energy regime but negligible for lower energies.

In the case where the generation of the asymmetry is extended to the DM sector, the new mechanisms responsible must comply with an adapted version of the Sakharov criteria:

- C-symmetry and CP-symmetry must be violated. C-symmetry violation ensures that interactions that produce more baryons/DM particles than anti-baryons/anti-DM particles are not counterbalanced by the charge conjugated reaction. CP-violation is similarly necessary because otherwise left-handed baryons/DM particles would be produced in equal amounts with right-handed anti-baryons/anti-DM particles and vice versa.

- Interactions must be out of equilibrium, because otherwise processes increasing baryon/DM number would be counterbalanced by reverse processes decreasing baryon/DM number.

The last Sakharov criterion;

- Baryon number B must be violated, for it to be possible to produce an excess of baryons over anti-baryons

can be omitted if the DM itself is viewed as carrying baryon number.

Models of *cogenesis* generally use modifications of existing lepto- and baryogenesis models that incorporate a concurrent generation of a DM asymmetry. *Darkogenesis* theories mimic successful features of existing baryogenesis scenarios, and focus on the communication of the asymmetry in the dark sector to the visible sector by the same kinds of transfer mechanisms as mentioned previously. Most constraints on darkogenesis are derived from the subsequent transfer of the asymmetry rather than from the mechanism of generation itself.

When an asymmetry has been established in both sectors, the mechanism communicating the asymmetry between sectors must decouple. For sphalerons this happens at the electroweak scale, while for higher dimension operators the scale at which the interactions decouple is set by the mass of the force mediator. This will result in separately freezing in the asymmetries of the two sectors, hence restoring the separate $B - L$ and D symmetries. If the dark sector was thermalized during the process of asymmetry generation, the symmetric component must efficiently be annihilated away so as to leave only (or almost only) the asymmetric component. If the symmetric abundance is not annihilated, the asymmetric component will be "resting on top" of an approximately 10^{10} times larger symmetric component, since the cosmological baryon asymmetry is of this order, $\eta = n_B/n_\gamma \approx 6 \times 10^{10}$.

The annihilation of the symmetric DM abundance is intimately related to the concept of hidden sectors, where the DM sector is envisioned to have a rich structure with multiple DM states and dark forces. The removal of the thermal DM abundance is only possible either through direct annihilation to light mediators, or through mediators that are heavier than the DM. These two interactions are shown in Figure 5.

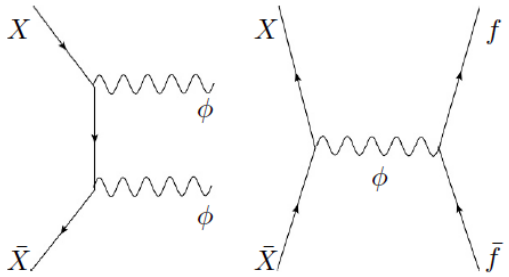


Figure 5: Processes for removing the thermal symmetric DM component. X $\bar{\text{X}}$ can annihilate to light force mediators ϕ, or through a heavier state directly to SM f $\bar{\text{f}}$. From Ref. [12].

It can be shown that an annihilation cross section $\sigma v \geq 10^{-25}$ cm^3/s is needed to sufficiently deplete the symmetric DM component, and that a cross section this size cannot be obtained for a mediator particle (consistent with collider constraints) of the weak scale or heavier. As a result, direct annihilation to light states in the DM sector is preferred for removing the symmetric component. This is analogous to the visible sector, where the electromagnetic force ensures efficient removal of excess positrons and anti-baryons, leaving only the asymmetric lepton and baryon components. By extension, the most natural way for DM to annihilate is to dark states. If these states are stable, they will remain as dark radiation today. Alternatively, the dark force mediators might decay to SM particles. ADM models thus naturally incorporate hidden sectors with DM self-interactions. These sectors may contain structure that is much more complex than the necessary minimum to deplete the symmetric abundance.

7 Dark Matter Detection

Dark matter is searched for and probed in several types of experiments, that each provide different and complementary information regarding the particle nature of DM.

The dark matter's cosmological stability, abundance and distribution, its interactions, decay and mass are all being explored experimentally as well as theoretically. Because DM may have non-gravitational interactions with any of the known particles as well as other dark particles, the different kinds of experiments are characterized by the type of interaction they are sensitive to. This is illustrated in Figure 6 and will be elaborated upon in the following sections along with an examination of the techniques involved with the various experimental approaches. The following sections will also contain a description of the constraints that can be placed on the different classes and specific candidates of DM previously considered in this report.

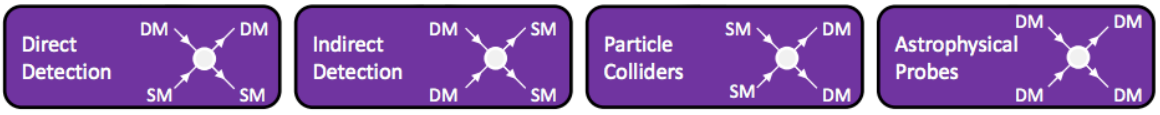


Figure 6: Schematic overview of the types of interactions that direct detection, indirect detection, particle colliders and astrophysical probes are sensitive to. Adapted from Ref. [13].

7.1 Direct Measurements

Question for this subsection: is all that I have indicated as applicable to DM in general really general or is some just applicable WIMPs?

The basic methodology of direct detection experiments is to search for rare events that might be the signature of DM, namely the scattering of DM from the galactic halo off a target nucleus contained within the experimental instruments. When the DM particle scatters off the target it imparts a small amount of energy in the form of a nuclear recoil [10] $E_{recoil} \sim 1 - 100$ keV. This energy is, in most cases, then converted to another form in the process of measurement, such as thermal motion, electronic ionization, scintillation light emission, or even sound. The rate of candidate nuclear recoils is measured from the response of these secondary modes and, subsequently, is converted into a cross section for DM-nucleon interactions. The expected rate is usually less than [14] 1 per kg per day. The determination of a limit on the cross section thus requires knowledge of effects of nuclear physics, astrophysical properties of the DM (density and velocity distribution in our galaxy) and the conversion to the secondary energy forms of the nuclear recoil. The experimentally determined scattering rate and cross section can then be compared to values predicted based on existing models.

Direct detection involves the construction of deep underground particle detectors to directly register the interactions of DM particles moving through the apparatus. This is necessary to avoid background noise from cosmic ray interactions as effectively as possible. Cosmic ray interactions with terrestrial particles can produce energetic neutrons that mimic closely the DM when they come in contact with the detector. A powerful way of discriminating between neutrons and DM particles is that neutrons tend to interact multiple times in the detector and typically closer to the surface of the detector material, while DM signals should consist of single hits and be uniformly distributed in the material. The experiment must also be shielded from the decay products of radioactivity in the environment and in the materials of the experiment itself. An alternative method to handling background noise exploits the fact that the Earth is moving through the DM in our galaxy, creating a "DM wind". This wind is

expected to cause a small annual modulation in the rate of candidate scatterings, as well as a daily modulation. However, if a modulation is detected it will be necessary to show that no such modulation is present in the background. Direct detection experiments are insensitive to strongly interacting DM, because this would be stopped in the atmosphere, earth or shielding of the experiment itself.

Experiments can be sensitive to both spin-independent (SI) interactions and spin-dependent (SD) interactions. For a DM particle with equal coupling to protons and neutrons the SI scattering cross section scales with the square of the atomic mass of the target nucleus, $\sigma_{SI} \propto m^2_{nucleus}$. The sensitivity to SI dark matter can thus be improved by using heavier nuclei as targets. On the contrary, the cross section of SD dark matter increases with the total nuclear angular momentum J, $\sigma_{SD} \propto J(J+1)$, which is considerably more difficult to increase than the atomic mass. Consequently, current experiments are more sensitive to SI dark mater than to SD dark matter. Measurements of the SD interactions are usually divided into proton and neutron couplings, as in Figure 8.

A confirmed signal from direct detection experiments would prove the presence of DM in our galaxy, while further study of the signal with several experimental targets could enable a determination of the DM mass, the forms of interactions it has with SM particles and provide information about the distribution of DM in our galaxy.

7.1.1 WIMP Direct Detection

In Figures 7 and 8 are shown limits on SI and SD WIMP-nucleon scattering cross sections. Thus far, only three direct detection experiments claim to have observed a potential dark matter signal. The favored regions are shown in Figure 7. The DAMA/LIBRA experiment has observed in 14 years of data a 9.3σ annual modulation that can be interpreted as a 10 GeV WIMP [14]. Other excess events at low recoil energy have been observed by CoGeNT, CDMS-Si, and CRESST, although CRESST with an upgraded detector no longer finds an unexplained excess in their rate [14]. If these events are interpreted as WIMP scattering, the data yield cross sections that range from $few \times 10^{-40}$ cm^2 to 10^{-42} cm^2 at masses that range from 5 to 20 GeV. This is a smaller mass than usually expected for WIMP dark matter. However, the DM interpretations of these experiments are not completely consistent with each other under the standard elastic scattering hypothesis. Furthermore, these observations have lost a great deal of potency due, especially, to the very stringent constraints recently provided by the LUX collaboration. LUX has obtained constraints on SI WIMP-nucleon scattering cross sections as small as $\sigma_{SI} \lesssim 10^{-45}$ cm^2, a limit which cuts definitively under the favored regions (as is evident from Figure 7). For SD WIMP-neutron scattering cross sections, the strongest constraints are provided by XENON-100 with $\sigma_{SD} \lesssim few \times 10^{-40}$ cm^2. Finally, in the case of SD WIMP-proton scattering, the most stringent limits are provided by the Ice Cube experiment with $\sigma_{SD} \lesssim 10^{-40}$ cm^2 (model-dependent).

Neutralino DM can elastically scatter with quarks either through t-channel CP-even Higgs exchange, or through s-channel squark exchange. The diagrams of these interactions are shown in Figure 9. The neutralino also has loop-level interactions with gluons that contribute to its scattering cross section with nucleons. The scattering cross section of a ~ 100 GeV MSSM neutralino off a nucleon is generally expected to reside in the range [10] $\sigma_{\tilde{\chi},n} \sim 10^{-46} - 10^{-41}$ cm^2. However, for a reasonable choice

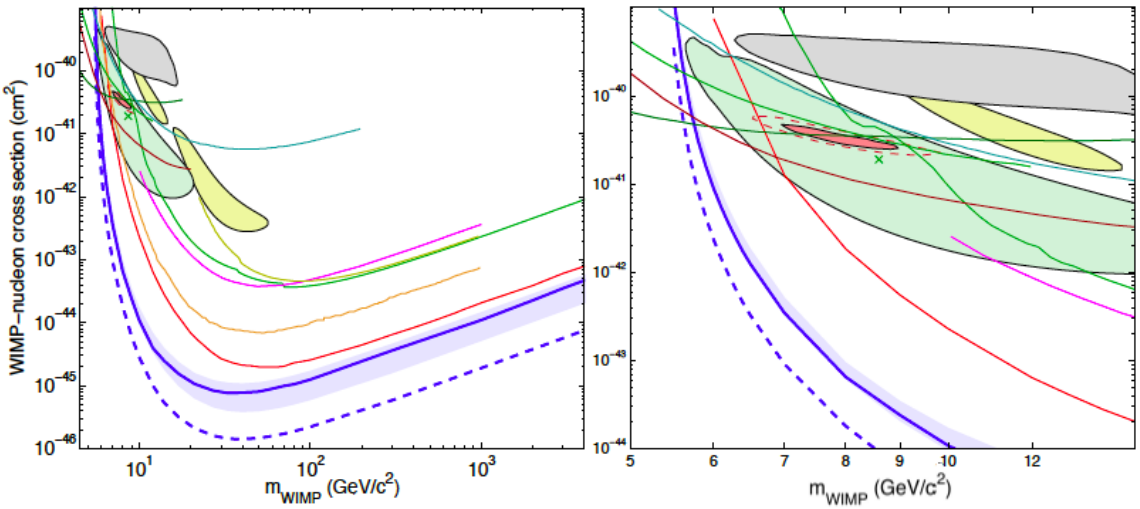


Figure 7: Spin-independent WIMP-nucleon scattering cross section limits, including closed contours showing hints for low-mass WIMP signals, as of February 2014. Left: The LUX 90% confidence limit (solid blue line) and 300-day projected sensitivity (dashed blue), with the $\pm 1\sigma$ variation from repeated trials (blue shaded). Limits from Edelweiss II (dark yellow line), CDMS II (green line), ZEPLIN-III (magenta line), CDMSlite (dark green line), XENON10 S2-only (brown line), SIMPLE (light blue line), and XENON100 100 live-day (orange line) and 225 live-day (red line). Right (zoom): The LUX limit (solid blue line), limits from low threshold re-analysis of CDMS II data (upper green line), allowed regions from CoGeNT (light red shaded), CDMS II silicon detectors (green shaded) and region centroid (green X), CRESST II (yellow shaded), and DAMA/LIBRA (gray shaded). From Ref. [15].

of parameters the cross section can even reach zero. Specifically, in the mSUGRA scenario the sign(μ) parameter is usually expected to yield $+$, to accommodate anomalies. If this prejudice is released, allowing sign(μ) $= -$ can result in cancellations making the scattering cross section extremely small without fine-tuning. Nevertheless, accepting the experimentally motivated condition sign(μ) $= +$, the discovery of the Higgs particle, lack of positive signals from the LHC, and null results from direct detection experiments, puts mSUGRA in considerable tension with recent experimental data. This has resulted in mSUGRA becoming increasingly disfavored. MSSM models that are to less extent constrained remain compelling even considering these new experimental bounds [13]. Hence, neutralino DM is still an attractive candidate, however, it is likely to exist within a framework that is somewhat more complex than mSUGRA.

B^1 Kaluza-Klein dark matter of the UED framework can scatter off quarks through s-channel exchange of KK quarks and t-channel Higgs boson exchange [10]. The diagrams for these interactions are shown in Figure 9. The spin-independent scattering cross section of a ~ 1 TeV B^1 particle off a nucleon is expected to reside in the range [4] $\sigma_{B^1 n,SI} \sim 10^{-47} - 10^{-44}$ cm^2. The spin-dependent scattering cross section of a ~ 1 TeV B^1 particle off a nucleon is expected to be [4] $\sigma_{B^1 n,SD} \sim 10^{-43} - 10^{-40}$ cm^2. For both the SI and SD case, a significant part of the range of the scattering cross section resides below current experimental limits.

In general, neutralino and KK dark matter nicely evade current direct detection

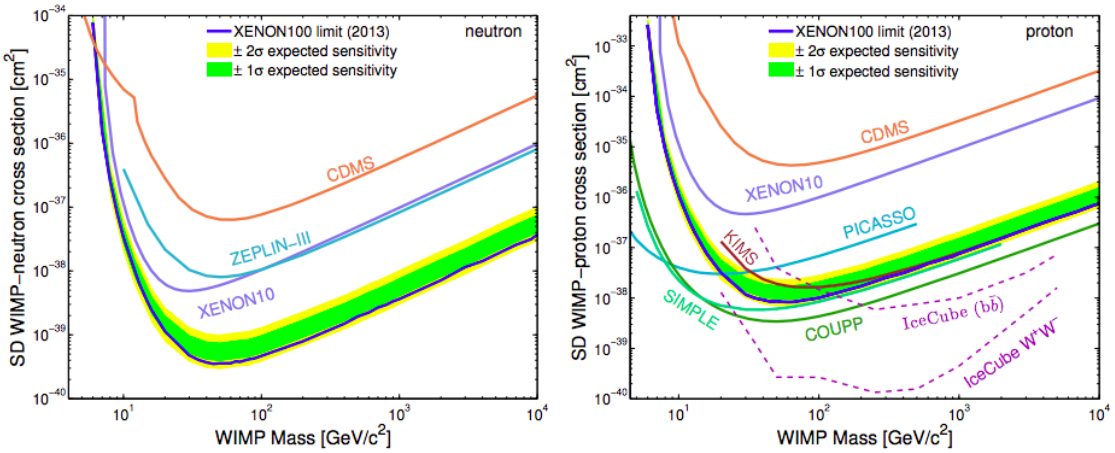


Figure 8: Spin-dependent WIMP-nucleon scattering cross section limits, as of summer 2013. Left: WIMP-neutron cross section limits from CDMS, ZEPLIN-III, XENON10, and XENON100 with $\pm 2\sigma$ and $\pm 1\sigma$ expected sensitivities indicated. Right: WIMP-proton cross section limits from CDMS, XENON10, PICASSO, KIMS, COUPP, SIMPLE, and XENON100 with $\pm 2\sigma$ and $\pm 1\sigma$ expected sensitivities indicated, compared with the model-dependent Ice Cube results. From Ref. [13].

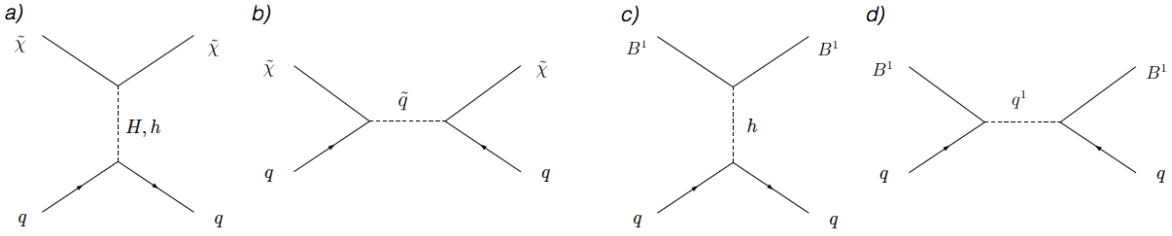


Figure 9: Feynman diagrams of WIMP DM interactions with quarks. To the left are shown diagrams of neutralino DM $\tilde{\chi}$ interactions with quarks q, a) via CP-even Higgs H,h exchange and b) via squark $\tilde{q}$ exchange. To the right are shown diagrams of KK dark matter B^1 interactions with quarks q, c) via Higgs boson h exchange and d) via KK quark q^1 exchange. Adapted from Ref. [10].

limits owing to their very small predicted scattering cross sections with nucleons. This, however, is not a universal feature of WIMPs. In fact, the two candidates discussed above represent somewhat special cases of particularly low direct detection rates. Many generic WIMP models predict scattering cross sections with nuclei that are several orders of magnitude greater than is allowed by current limits.

The results presented in Figures 7 and 8 use the "Halo-Dependent" data comparison method. The observed rate in a particular direct detection experiment depends on three main elements: the detector response to potential WIMP collisions, the WIMP-nucleon cross section and WIMP mass, and the local DM density and velocity distribution. In the "Halo-Dependent" analysis of the data, all three elements are fixed, except for the WIMP mass m and a referential scattering cross section σ_{ref}. Usually the Standard Halo Model [14] is assumed for the distribution of the DM. The constraints are then plotted in the (m, σ_{ref}) plane as in Figures 7 and 8. If the WIMP in question constitutes only a fraction R of the local DM density, the direct detection

limits must be multiplied by $1/R$. The "Halo-Dependent" method typically assumes $R = 1$.

The "Halo-Independent" data comparison method fixes the first two elements of the rate, again with the exceptions of the WIMP mass and the referential scattering cross section, but does not make any assumptions concerning the DM density and velocity distribution. In this way, the uncertainties in the characteristics of the galactic dark halo do not affect the constraints derivable from the experiment. For a particular DM candidate the interaction rate at one particular recoil energy depends for any experiment on the same function of the referential cross section and DM distribution $\sigma_{ref}\rho\eta(v_{min}, t)/m \equiv \tilde{\eta}(v_{min}, t)$, where v_{min} is the minimum speed a WIMP must have to communicate the specific recoil energy to the target. Thus, all rate measurements and constraints can be mapped onto measurements of and constraints on the unique function $\tilde{\eta}$ for a fixed WIMP mass and be plotted in the $(v_{min}, \tilde{\eta})$ plane. For experiments to be compatible, they must measure the same function $\tilde{\eta}$. This type of analysis has so far indicated that one of the potential direct DM detection signals (DAMA/LIBRA, CDMS-Si, CoGeNT) at a time could be compatible with all negative results for particular DM candidates [14].

Direct detection is a very active field of research, in which astounding progress has been made in the last three decades, with sensitivities to WIMPs doubling roughly every 18 months. Unfortunately, this rate of progress can not continue unimpaired, but must encounter considerable difficulties in the nearby future due to the interference of neutrinos with experiments. When sensitivities can be pushed down approximately four orders of magnitude with respect to the LUX limit, experiments will become sensitive to the very weak interactions of neutrinos. Thus, if the WIMP-nucleon scattering cross section is smaller than that of neutrinos and nucleons, the signal will become obscured by a neutrino background.

7.1.2 Axion Direct Detection

Direct detection experiments typically search for axions by exploiting two types of detection mechanisms. One relies on the Primakov effect, whereby an axion can be converted into a photon via coupling to the electric field of the crystal within the experimental instruments. The process can be represented as, $A\gamma^* \to \gamma$, where γ^* is provided by the background electric field of the crystal. Depending on the orientation of the crystal lattice with respect to the incoming flux of axions, it is possible to significantly enhance the signal through Bragg diffraction **how does this work?**. This mechanism is related to the axion-photon coupling, $g_{A\gamma}$. Axions can also be detected through the axio-electric effect, which is analogous to the photo-electric effect with the absorption of an axion instead of a photon. An incoming axion will generate an electron recoil, which is then recorded by the detector. This mechanism is related to the axion-electron coupling, g_{Ae} [16]. Current constraints on the couplings of axions with photons and electrons are shown in Figures 10 and 11, respectively. **Which bounds are the best? How is it going for the axion model? Why is mass range in plots so large?**

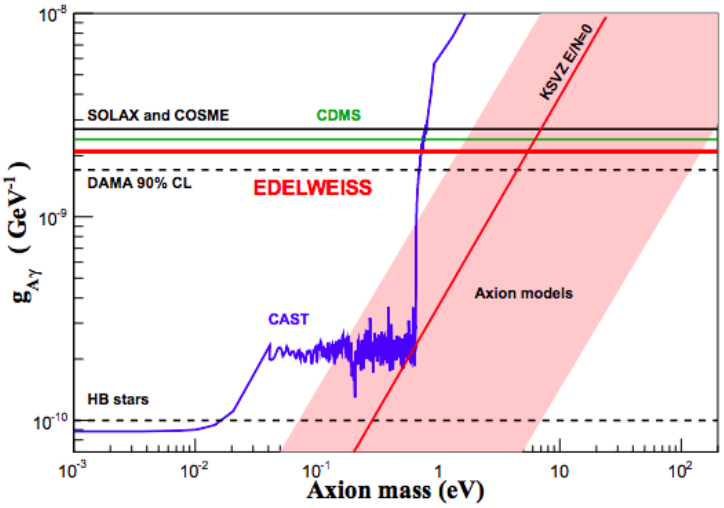


Figure 10: Limits on axion-photon coupling $g_{A\gamma}$, as of July 2013. 95% CL limit from Edelweiss-II (red), limits from SOLAX, COSME, CDMS and DAMA (90% CL). Also shown is the CAST limit and indirect bounds from horizontal branch (HB) stars. The light red band labeled "Axion models" represents the prediction of typical theoretical models. The red solid line inside this band represents the KSVZ (Kim-Shifman-Vainstein-Zakharov) model. From Ref. [16].

7.1.3 ADM Direct Detection

ADM scattering with nuclei through a dark force and self-interactions give rise to a broad range of experimental signatures. In many ADM models, especially those that include a light dark force, large scattering cross sections are expected in direct detection experiments. The dark force to which the DM annihilates to deplete its symmetric abundance may also mediate scattering off nucleons. Sufficient annihilation places a lower bound on the coupling between the DM and the mediator. A lower bound on the scattering cross section of DM off nucleons through this mediator can then be obtained by requiring thermal equilibrium at some point in the early universe [12]

$$\sigma_{n,X} \gtrsim 10^{-48}\ \mathrm{cm}^2 \left(\frac{m_X}{\mathrm{GeV}}\right)^4 \left(\frac{\mathrm{GeV}}{m_\phi}\right)^6 \left(\frac{\mu_n}{0.5\ \mathrm{GeV}}\right)^2 . \tag{45}$$

Here μ_n is the DM-nucleon reduced mass. Scattering off electrons when the particle mediating the scattering is heavier than the dark matter particle implies [13] $\sigma_{e,X} \gtrsim 10^{-41}$ cm^2 for 1 GeV dark matter.

7.2 Indirect Measurements

Is everything in this section relevant to all candidates or is some only relevant to WIMPs? The basic technique of indirect searches is to look for the standard model annihilation or decay products of dark matter. The flux of this radiation is proportional to the annihilation rate, which in turn depends on the square of the DM density, hence, for obtaining significant fluxes, it is advantageous to probe regions with large DM densities. The dark matter sources probed in indirect detection experiments are the dark haloes of our own and other galaxies, as well as dark matter accumulated within the Sun or Earth. Indirect detection experiments are sensitive to

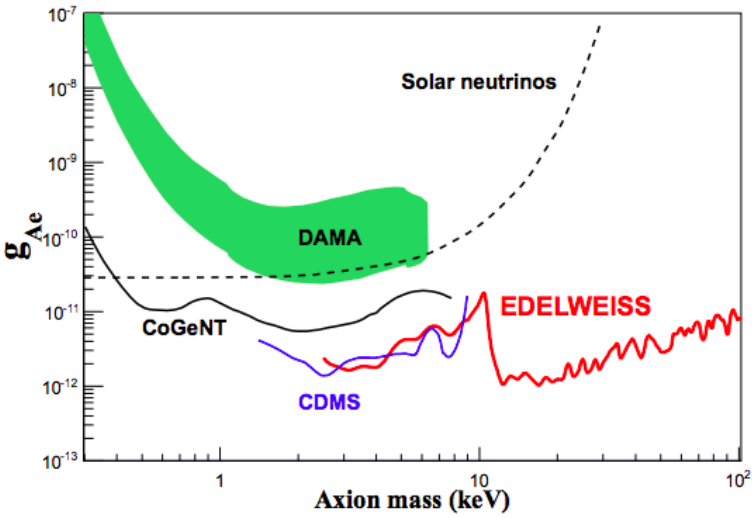


Figure 11: Limits on axion-electron coupling g_{Ae}, assuming the local dark matter halo of our galaxy is made entirely of axions, as of July 2013. Shown is the favored region from DAMA (green), constraints set by CoGeNT (black) and CDMS (blue), and indirect bound from the solar neutrino flux measurement (dashed). From Ref. [16].

interactions with all SM particles, however, astrophysical backgrounds have a great influence in the experiments and knowledge of these is necessary to distinguish signals from background. The analysis is also subject to uncertainties in the density and velocity distributions of galactic dark matter.

This type of detection is only sensitive to DM that annihilates or decays presently, hence if the DM is exclusively asymmetric it is not detectable through indirect searches.

7.2.1 WIMP Indirect Detection

The annihilation or decay products searched for from WIMPs are high energy neutrinos produced by WIMPs captured within the Sun or the Earth, and photons, positrons and antiprotons produced in galactic halos.

As the Sun and Earth move through the dark matter halo of the Milky Way, WIMPs pass through these astronomical bodies and occasionally scatter off the baryonic matter that make up the bodies. Through scattering, the WIMPs may be slowed to under escape velocity and become gravitationally bound to the object. The capture rate Γ_C is proportional to the scattering cross section and the local DM number density, [14] $\Gamma_C \propto \sigma_S n$ (where the subscript S denotes scattering and A will denote annihilation). This is where uncertainties from the astronomical characteristics of DM is introduced into the experiment. The detected annihilation products provide information about the annihilation rate Γ_A, which is related to the annihilation cross section and the number of captured WIMPs as [14] $\Gamma_A \sim \sigma_A N^2$, where $N = \Gamma_C t$, hence annihilation rates are greatly enhanced in regions where DM accumulates. Of the annihilation products, only neutrinos escape the astronomical bodies due to their very weak interactions. These neutrinos are usually much more energetic than neutrinos otherwise produced in astronomical bodies. To make a prediction of the neutrino flux, one must then

construct a model for the capture mechanism, the annihilation cross section, and the production of neutrinos in annihilation.

Neutrino telescopes, which are the detectors used to measure the neutrino flux, consist of large volumes of instrumented water or ice on or beneath the surface of the Earth. It is an asset of this type of experiment that if a signal is detected originating from the Sun all astronomical backgrounds can be eliminated based on the motion of the source. The best constraints on neutrinos from the Sun are provided by the IceCube experiment. In the limit of equilibrium, where the annihilation rate compensates the capture rate, the neutrino flux only depends on the capture rate, which in turn depends on the scattering cross section of WIMPs with baryons, thus allowing for a direct comparison with direct detection experiments, as in Figure 8.

The detection of photons has the advantage of revealing the spatial distribution of the sources. This is due to the fact that the Universe is completely transparent to photons below 100 GeV [14]. Gamma-ray astronomy is done using both ground- and space-based telescopes. Annihilation of dark matter can produce monochromatic photons through, [14] DM DM $\rightarrow \gamma\gamma$ (or γZ) with energy approximately equal to the mass of the DM particle. Detection of this monoenergetic spectral line would be a "smoking gun" signature of DM. Unfortunately this process is highly suppressed, but secondary photons, especially from pion decay $\pi^0 \rightarrow \gamma\gamma$, would be produced with a spectrum cutoff at the WIMP mass. Thus, a cutoff in the observed spectrum would be a signature of dark matter, though not exclusively. There is a background from astrophysical objects that also have cutoffs in their spectra, because there is a limit to the energy with which photons can be produced in the objects.

As with neutrinos, it is favorable to search in regions of high DM density to obtain a greater flux of photons, but in this case astronomical bodies are inappropriate sources, since gamma-rays are absorbed before escaping these bodies. Instead the favored regions are the galactic center, DM clumps, dwarf galaxies and other galaxies or galaxy clusters. Dwarf galaxies are the most DM dominated structures observed in the Universe. The FermiLAT cooperation provides limits on the annihilation cross section of thermal WIMPs based on measurements of the photon spectrum of 15 dwarf galaxies. These limits are shown in Figure 12. Together with the lower limit on the annihilation cross section at freeze-out for a thermal WIMP, imposed by the observed relic density, the FermiLAT results constraint the WIMP mass to be [14] $m > 20$ GeV (from the $\tau^+\tau^-$ and $\mu\bar{\mu}$ modes).

The galactic center is also a preferable region for indirect detection through photons, although the amount of dark matter at the galactic center is uncertain. The NFW (Navarro, Frenk and White) model, which is based on numerical simulations of structure formation with cold DM only, provides a scale independent density profile that goes as $1/r^3$ at large distances from the galactic center and as $1/r$ close to the center [14]. This is a "cuspy profile", which is expected to be modified by the effects of baryons close to the center. Models based on observed rotation curves of galaxies yield a "cored profile" rather than a cusp. Such a density profile becomes constant close to the galactic center. The scale factor of any model is fixed by the rotation speed of the Sun.

Several old and new gamma-ray signals have been detected from the galactic center that might be contributed to DM annihilation. The INTEGRAL satellite detected a

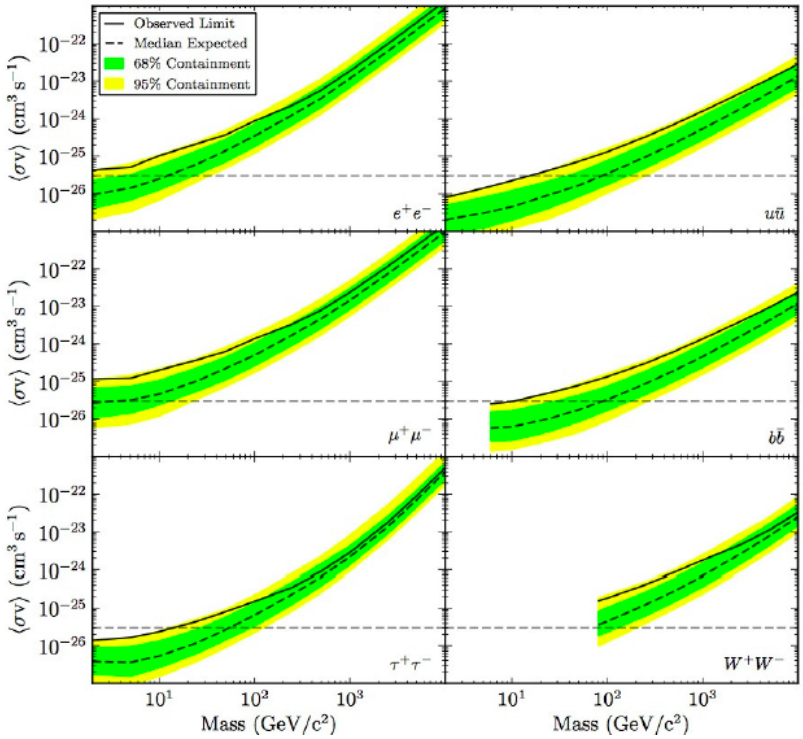


Figure 12: Fermi upper limits on the DM thermally averaged annihilation cross section $\langle\sigma_A v\rangle$ from 15 stacked dwarf galaxy images, assuming exclusive annihilation in each of the modes shown. The lower limit on $\langle\sigma_A v\rangle$ at freeze-out for thermal WIMPs is shown as a horizontal dashed line at 3×10^{-26} cm^3/s. From Ref. [14].

511 keV signal in 2002 originating from the galactic center, which was due to annihilation of non-relativistic positrons e^+ with electrons e^- almost at rest [14]. Initially the emitting region seemed spherically symmetric, as expected for a DM signal, and special DM candidates were proposed with e^+e^- as a decay or annihilation product to explain the signal. However, in 2008 INTEGRAL revealed that the region is not spherically symmetric, and found evidence consistent with a binary star system being the positron source, hereby decreasing the motivation to consider the 511 keV line as a DM signal.

The WMAP haze is an excess of photons in the microwave spectrum originating from the galactic center, which was discovered in 2003 by D. Finkbeiner [14]. The signal can be identified either as synchrotron radiation from astrophysical sources or as a WIMP annihilation product. However, the signal has since 2009 been considered to originate from the "Fermi Bubbles". These are two large structures emitting gamma-rays that might have been formed in an early period of jet-like activity of the black hole at the galactic center.

In 2011 a spatially extended GeV photon excess was found by Hooper and Linden by subtracting all known contributions from the Fermi data [14]. The excess peaks at 2-3 GeV and is emitted from the galactic center. The signal can be interpreted as DM particles with mass of 7-12 GeV annihilating to $\tau^+\tau^-$ (among other leptons), or DM particles with mass of 22-45 GeV annihilating to quarks with an annihilation cross section close to that needed to correctly produce the thermal relic density. In both cases the galactic DM density profile must be cuspy, to ensure sufficient annihilation. Alternatively, the GeV excess can also be explained by unresolved millisecond pulsars,

which are rotating neutron stars in a binary system that have been spun up to a period of 1-10 milliseconds through accretion from their partner star. These emit X-rays and gamma-rays, possibly from the accreting matter, and their distribution close to the galactic center is unknown, as is the emitted photon spectrum. Hence, many assumptions about either source must be made to fit the data.

In 2012 a 130 GeV line was found with 3.5σ significance in the FermiLAT data by C. Weniger and collaborators [14]. This spectral line can be contributed to DM annihilation into $\gamma\gamma$, besides a hint of a 111 GeV line was also found, which might correspond to annihilation of the same particles to $Z^0\gamma$. However, no evidence of the 130 GeV line has been found in other regions of high DM density. Conversely, it has been measured emanating from regions that do not contain significant amounts of dark matter; in the vicinity of the Sun, and in Earth's Limb (the edge of the disk of the Earth, where gamma-rays are produced by cosmic rays). This suggests that the spectral line is an effect of the detector. Another indication that the line does not come from DM annihilation is that its accumulated significance decreases with time.

Positrons and antiprotons would be produced in DM annihilation in equal amounts as electrons and protons. Positrons and antiprotons are an important potential signal of WIMP annihilation, because there is not much antimatter in the Universe. Unfortunately, positron rays do not travel in straight lines and quickly (within a few kpc) loose energy to synchrotron radiation from travelling in the magnetic fields of the galaxy, as well as to inverse Compton scattering interactions (where a high energy e interacts with a γ with much smaller energy to produce a lower energy e and a higher energy γ). Antiprotons are impeded by convective mixing **what is that?** and spallation. They propagate further out from the galactic center than do positrons, but still only reach a fraction of the size of the galaxy.

The PAMELA experiment reported in 2008 an excess in the positron fraction $e^+/(e^+ + e^-)$ in the 10-100 GeV range [14]. This measurement was consistent with the excess that had been measured by balloon experiments since the 1980's, and the result was confirmed by FermiLAT and more recently by AMS-02. The excess indicates the nearby existence of primary sources (outside the Earth's atmosphere) of high energy positrons, such as pulsars or annihilating WIMPs. It is important that no corresponding excess of antiprotons has been measured, since this implies that if DM is responsible for the positron excess, then DM only annihilates (or decays) to leptons and not quarks. This may either be because the DM carries lepton number **if it carries lepton number can it not decay into quark-antiquark pairs?** or because of kinematics **how?**. No cutoff for the positron excess was observed by PAMELA or AMS, which could indicate the mass of the dark matter. Several possible WIMP annihilation processes exist that may account for the excess, if assumptions are made about the mass and annihilation rate of the DM. Models in which the excess positrons are produced in DM decays can also be constructed, again with certain assumptions about the DM properties.

7.2.2 ADM Indirect Detection

Though DM may consist primarily of its asymmetric component today, a small relic symmetric abundance may also be present, which can annihilate and produce signals in the CMB and in indirect detection experiments. Because a larger annihilation cross

section depletes the symmetric component, leaving less of it to annihilate today, the implication is a lower constraint on the annihilation cross section. Depending on the mass of the DM, the CMB places the constraint [12] $f\langle\sigma v\rangle \gtrsim 10^{-25}$ cm^3/s, where f is the ionizing efficiency of the radiation from the DM. This constraint is valid if the DM retains its asymmetry until today.

No indirect detection of axions? Do they not annihilate? Do antiaxions exist?

7.3 Colliders

Dark matter may be produced in the collisions of standard model particles, given that the reaction is sufficiently energetic (or, correspondingly, that the dark matter is sufficiently light). DM particles escape the detectors at colliders, and are thus characterized by missing transverse energy. Particle colliders are necessarily affected by SM backgrounds that may obscure the signal. Also, since DM particles escape the detectors, it is impossible to distinguish a signal produced by a DM particle with a lifetime $\tau \sim 10^{-7}$ s from one with $> 10^{17}$ s as required to yield the correct relic density. A strategy that can be applied in the search for DM at colliders is assuming knowledge of the entire particle model the DM belongs to, along with its interactions with particles that are directly observable in the detectors. For example, supersymmetry predicts the production of pairs of squarks and gluinos, which decay through some cascade chain, eventually producing neutralino WIMPs that can be registered as missing energy [4]. Hence, the signature of neutralino DM at a collider is the observable particles of the decay chain known to end up in neutralinos, together with the missing energy corresponding to the DM particles themselves.

7.3.1 WIMP Detection at the LHC

Does any of this apply to axions, ADM as well? Another method to search for DM at colliders relies on direct pair production [14]. Reactions such as $SM\ SM \to \chi\bar{\chi}$ are undetectable, however, related reactions where a visible particle is emitted either by the initial or intermediate SM particles can be characterized by the observable particle and missing energy. If the one visible particle emitted is a photon, it is a "monophoton" event, if it is a gluon, it is a "monojet" event. Thus far the constraints obtained from monophoton, monojet, and other mono-particle events have been derived using Effective Field Theory.

Effective Field Theory allows one to avoid considering a specific ultraviolet completion of the DM model, by assuming effective couplings between DM particles and quarks or gluons [17]. It also has the advantage of facilitating comparison between different types of experiments. The effective operators mimic the effect of heavy particles in the reaction. The operators are non-renormalizable, thus the theory is only valid at energies that are small compared with the scale of the process M_*. If a reaction is mediated by a particle of mass M with coupling λ, the mediator is assumed to be heavy $M \gg Q$ with respect to the momentum transfer Q of the LHC partonic reaction **what is this?**, so its propagator reduces to a constant $\lambda^2/M^2 = 1/M_*^2$ [17]. In this limit interference between operators is neglected, and the approach does not extend to light mediators.

The same effective couplings used to obtain limits from collider experiments can be applied to compute the WIMP interaction with nuclei in direct detection experiments, and the results can be compared in plots as in Figure 13. This type of plots should be read with caution, however. Notice that while it is valid to include the direct detection limits when presenting the limits from the LHC, the opposite is not necessarily correct. A mediator that is heavy in comparison with the momentum transfer of a partonic reaction in the LHC, $Q \sim 100$ GeV, will also be heavy compared to the typical MeV momentum transfer in direct detection experiments. Hence, the requirement $M \gg Q$ is sure to hold for direct detection if it is true for the LHC reaction, but the reverse holds no such guarantee. Actually, a mediator that is heavy compared to direct detection might even be light enough to be produced at the LHC, and the analysis of the data from the LCH should then be completely different.

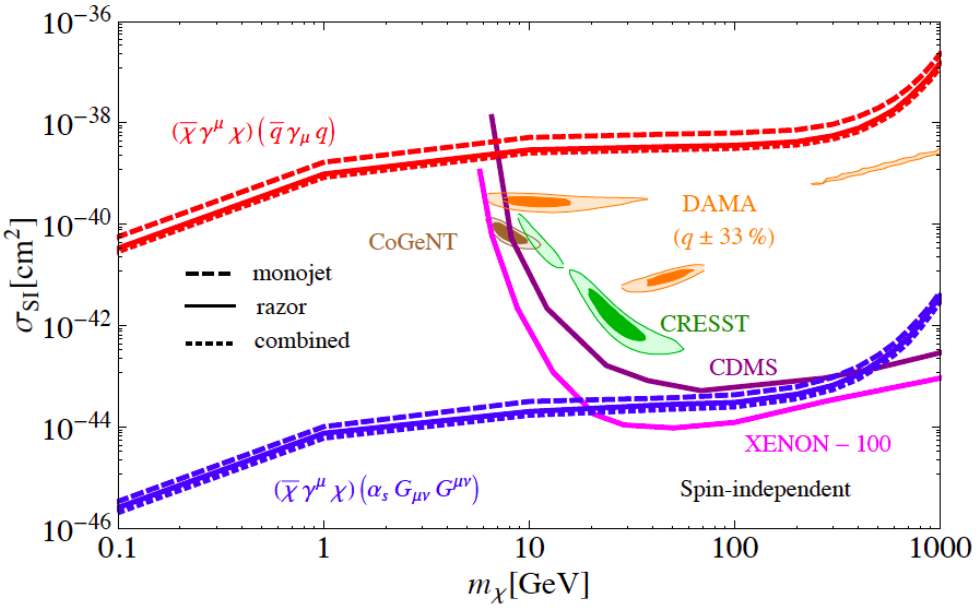


Figure 13: LHC bounds (monojet limits and others) on SI DM-nucleon scattering compared to direct detection limits. Constraints are shown from DM-quark coupling (red lines) and from DM-gluon coupling (blue). For DAMA and CoGeNT 90% and 3σ contours and for CRESST 1σ and 2σ contours are also shown. From Ref. [14].

7.4 Astrophysical Probes

Detection through astrophysical probes relies on possible self-interactions of dark matter, and the influence the presence of dark matter has on astrophysical systems. The caveat to this type of detection is that it is very dependent on the model chosen for the density and velocity distributions of DM, and a thorough knowledge of the astrophysical bodies used as probes is important to derive useful constraints. Because asymmetric dark matter can accumulate in relatively small regions, such as astronomical bodies, this type of probes are especially relevant to ADM.

7.4.1 ADM Astrophysical Observations

If ADM retains its asymmetry until today, it can accumulate in astrophysical objects and influence their evolution. Accumulated ADM with self-interactions produces different density profiles in dwarf galaxies and clusters of galaxies than does the standard WIMP scenario. WIMP DM, which carries little or no self-interactions, produces cusp-like density profiles, but observations imply that dwarf galaxies and clusters have a core of DM rather than a cusp. This structure problem is resolved for ADM because its self-interactions can transfer heat from the outer part of the halo to the inner part, flattening the density profile of the inner part of the halo.

The amount of ADM that is captured is proportional to the local DM density, the scattering cross section of the DM off the baryons in the object, and the depth of the gravitational potential well do to the object. Hence, astrophysical objects place important constraints on the ADM scattering cross sections off baryons.

Neutron stars are supported by Fermi degeneracy pressure. If ADM is bosonic, however, this degeneracy pressure does not apply to the DM, so that if the DM collected in the neutron star exceeds the Chandrasekhar mass, a black hole (BH) may form that could consume the neutron star if the BH grows at a greater pace than it evaporates. The existence of neutron stars thus constrains the ADM, placing a lower bound on the scattering cross section of ADM on nucleons. This constraint is plottet in Figure 14. Self-interactions play a significant role in this story as well, and can either relax or strengthen the constraint, depending on the sign of the self-interaction.

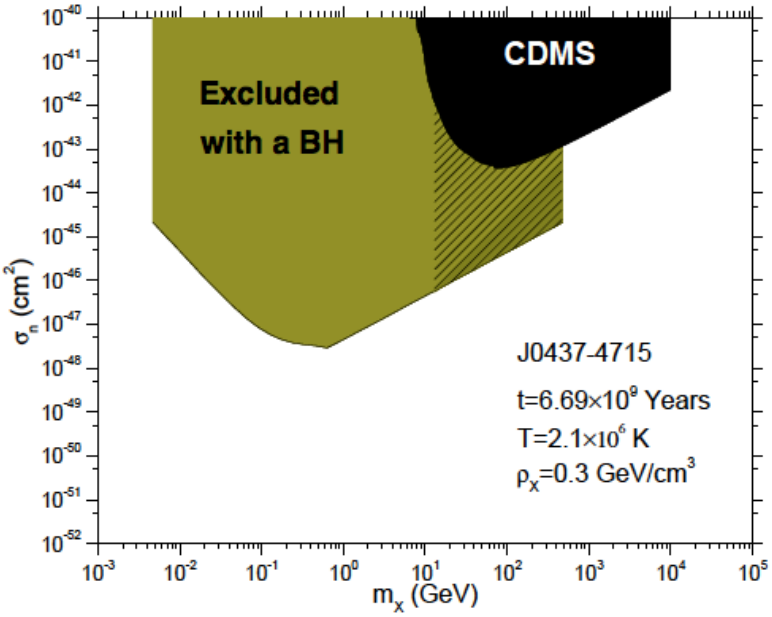


Figure 14: Excluded scattering cross section of ADM off a nucleon from BH formation in the neutron star J0437-4715. In the hatched region constraints are lifted, because the BH evaporates. For comparison, the constraint from the direct detection experiment CDMS-II is shown. t is the lifetime of the neutron star, T is its temperature and ρ_X is the DM energy density. Adapted from Ref. [12].

Low mass stars, with masses below $0.08 M_\odot$, evolve to brown dwarfs in usual stellar evolution, because the core never reaches a temperature where hydrogen burning is

possible. If a low mass star, with a mass greater than $0.08M_{\odot}$, captures a significant amount of ADM it too can become a brown dwarf, because the DM can influence the energy transport in the star in such a way that it cannot reach its main sequence. It has been shown that a spin-dependent scattering cross section of DM off nucleons $\sigma_{SD} \sim 10^{-37}$ cm^2 or a spin-independent scattering cross section of $\sigma_{SI} \sim 10^{-40}$ cm^2, taken with a capture rate boosted by 10^3 in comparison with that expected in the Sun, will cause a star with mass $0.08 - 0.1M_{\odot}$ to become a brown dwarf [12]. Lastly, accumulation of ADM in the Sun may modify its internal energy transport, and hence change its radiative history. This effect can also be present in stars with masses smaller than that of the Sun. α Cen B ($0.9M_{\odot}$) has been used as a probe of ADM and a constraint of $few \times 10^{-36}$ cm^2 was placed on the scattering cross section for ~ 10 GeV DM, assuming a DM density of 0.4 GeV cm^{-3} [12].

8 Alternative Models

When considering the astonishing amount of progress that has been made within DM detection, one might wonder at the fact that no DM signal has yet been confirmed. It is possible that the interactions of dark matter with visible matter are simply even weaker than currently detectable. Another possibility is that dark matter has no weak interactions at all, which leaves a particle that only interacts through gravity or no particle at all! Some alternative models assume this scenario and attempt to explain the effects usually contributed to dark matter by making alterations to the theory of gravity.

8.1 MOND

Modified Newtonian Dynamics (MOND) was first proposed in 1983 by Milgrom to explain the flat rotation curves observed in galaxies as a departure from the laws of gravity as described by general relativity [10]. MOND is a phenomenological model based on the idea that Newton's second law should be modified at galactic scales:

$$F = ma \times \mu(a), \tag{46}$$

where μ is extremely close to unity except for very small accelerations where μ behaves as $\mu = a/a_0$. Applying the modified second law of Newton to the gravitational force on a star of mass M outside of a galaxy in the small acceleration limit yields

$$a = \frac{\sqrt{GMa_0}}{r}. \tag{47}$$

Equating this with the centrifugal acceleration of a body in a circular orbit one finds a constant velocity curve dependent on the acceleration scale a_0,

$$v = (GMa_0)^{1/4}. \tag{48}$$

This result is in good agreement with observations at the scales of galaxies for a value of [10] $a_0 \sim 1.2\times10^{-10}$ m/s^2, without introducing dark matter into the system. For this value of a_0 MOND is undetectable in laboratories or solar system scale experiments. However, MOND is not able to address evidence such as the CMB anisotropies and large scale structures, because it is a phenomenological modification of Newtonian

dynamics and thus is not applicable to problems addressed by general relativity, such as the expansion history of the Universe. Efforts have been made to generalize MOND to a relativistic covariant theory, but the attempts have largely been unsuccessful. A notable exception is Tensor-Vector-Scalar gravity (TeVeS), which is a relativistically covariant theory that yields MOND in the weak-field non-relativistic limit. But TeVeS fails to describe the observed features of clusters of galaxies, specifically evidence from the Bullet Cluster cannot be explained without introducing some form of dark matter [14]. TeVeS requires 2-3 times more matter than accountable for in visible matter alone. Advocates of TeVeS propose the existence of "cluster baryonic dark matter", for example. However, once it is necessary to introduce some form of invisible extra matter, it becomes a question of preference which type of dark matter one considers more likely.

9 Outlook

Presently, particle candidates for dark matter are abundant, however, no compelling evidence exists in favor of any specific dark matter candidate. Further experimental investigations are paramount in determining the nature of dark matter. Within the next decades important progress will be made in the direction of experimental evidence. Direct detection experiments will move to the ton-scale, indirect detection will continue its rapid development, and the LHC with its full capacity will push into beyond the standard model physics. The respective types of dark matter probes will each provide different and complimentary information, and it is likely that all classes of experiments will be necessary to the conclusive identification of the dark matter particle. While collider experiments may measure a long-lived ($\tau > 10^{-7}$ s), weakly interacting particle, direct and indirect detection experiments will be able to test its cosmological stability ($\tau > 10^{17}$ s), distribution and abundance.

A confirmed signal will without doubt open the door to interesting new physics. Because most dark matter candidates are relics from the pre-BBN era, if a DM particle is discovered, it can be used as a cosmological probe to gain information about this epoch. A discovery could potentially confirm the existence of supersymmetry or extra dimensions, or we might reveal the presence of an axion field or asymmetric dark matter. It is even conceivable that what we uncover is an entire hidden sector with complex structure and self-interactions, or a combination of several candidates and the models they belong to.

Acknowledgements

I thank Maria Spiropulu and Cliff Cheung for excellent guidance. I would also like to thank Kathryn Zurek for taking time to discuss Asymmetric Dark Matter with me, and Sunil Golwala for his help in my study of direct detection experiments. Finally, I thank Cristian Peña and Javier Duarte for taking time to discuss Effective Field Theory with me.

References

[1] F. Zwicky, 2008, "Republication of: The redshift of extragalactic nebulae" (1933). Source: Gen. Relativ. Gravit. (2009) 41:207–224. DOI 10.1007/s10714-008-0707-4.

[2] G. Bertone, D. Hooper, J. Silk, 2008, "Particle Dark Matter: Evidence, Candidates and Constraints".

[3] Sanders, R. H., 2010, "The Dark Matter Problem: A Historical Perspective". Cambridge University Press.

[4] J. L. Feng, 2010, "Dark Matter Candidates from Particle Physics and Methods of Detection".

[5] M. Kamionkowski, 2007, "Dark Matter and Dark Energy".

[6] S. Carroll, 2014, "Spacetime and Geometry: An Introduction to General Relativity".

[7] E. Kolb, M. Turner, 1994, "The Early Universe".

[8] ATLAS Collaboration, 2012, "Observation of a new particle in the search for the Standard Model Higgs boson with the ATLAS detector at the LHC", Physics Letters B 716 1–29.

[9] P. A. M. Dirac, 1930, "On the Annihilation of Electrons and Protons", Mathematical Proceedings of the Cambridge Philosophical Society 26 03 361-375.

[10] D. Hooper, 2009, "TASI 2008 Lectures on Dark Matter".

[11] J. Preskill, M. Wise, F. Wilczek, 1983, "Cosmology of the Invisible Axion", Phys. Lett. B 120, 127-132.

[12] K. M. Zurek, 2013, "Asymmetric Dark Matter: Theories, Signatures, and Constraints".

[13] P. Cushman, C. Galbiati, D. N. McKinsey, H. Robertson, T. M. P. Tait *et al.*, 2013, "Snowmass CF1 Summary: WIMP Dark Matter Direct Detection".

[14] G. B. Gelmini, 2015, "TASI 2014 Lectures: The Hunt for Dark Matter".

[15] Matthew Szydagis, on behalf of the LUX collaboration, 2014, "A Detailed Look at the First Results from the Large Underground Xenon (LUX) Dark Matter Experiment".

[16] EDELWEISS collaboration, 2013, "Axion searches with the EDELWEISS-II experiment".

[17] G. Busoni, A. De Simone, E. Morgante, A. Riotto, 2013, "On the Validity of the Effective Field Theory for Dark Matter Searches at the LCH".